

# 1 A multi-model comparison of meteorological drivers of surface ozone 2 over Europe

3  
4 Noelia Otero<sup>1,3</sup>, Jana Sillmann<sup>2</sup>, Kathleen A. Mar<sup>1</sup>, Henning W. Rust<sup>3</sup>, Sverre Solberg<sup>4</sup>,  
5 Camilla Andersson<sup>5</sup>, Magnuz Engardt<sup>5</sup>, Robert Bergström<sup>5</sup>, Bertrand Bessagnet<sup>6</sup>,  
6 Augustin Colette<sup>6</sup>, Florian Couvidat<sup>6</sup>, Cournelius Cuvelier<sup>7</sup>, Svetlana Tsyro<sup>8</sup>, Hilde  
7 Fagerli<sup>8</sup>, Martijn Schaap<sup>9,3</sup>, Astrid Manders<sup>9</sup>, Mihaela Mircea<sup>10</sup>, Gino Briganti<sup>10</sup>, Andrea  
8 Cappelletti<sup>10</sup>, Mario Adani<sup>10</sup>, Massimo D'Isidoro<sup>10</sup>, María-Teresa Pay<sup>11</sup>, Mark  
9 Theobald<sup>12</sup>, Marta G. Vivanco<sup>12</sup>, Peter Wind<sup>8,13</sup>, Narendra Ojha<sup>14</sup>, Valentin Raffort<sup>15</sup>  
10 and Tim Butler<sup>1,3</sup>  
11

12 <sup>1</sup>Institute for Advanced Sustainability Studies e.V., Potsdam, Germany

13 <sup>2</sup>CICERO Center for International Climate Research, Oslo, Norway

14 <sup>3</sup>Freie Universität Berlin, Institut für Meteorologie, Berlin, Germany

15 <sup>4</sup>Norwegian Institute for Air Research (NILU), Box 100, 2027 Kjeller, Norway

16 <sup>5</sup>SMHI, Swedish Meteorological and Hydrological Institute, Norrköping, Sweden

17 <sup>6</sup>INERIS, Institut National de l'Environnement Industriel et des Risques, Verneuil en  
18 Halatte, France

19 <sup>7</sup>European Commission, Joint Research Centre (JRC), Ispra, Italy

20 <sup>8</sup>MET Norway, Norwegian Meteorological Institute, Oslo, Norway

21 <sup>9</sup>TNO, Netherlands Institute for Applied Scientific Research, Utrecht, the Netherlands

22 <sup>10</sup>ENE-National Agency for New Technologies, Energy and Sustainable Economic  
23 Development, Bologna, Italy

24 <sup>11</sup>Barcelona Supercomputing Center, Centro Nacional de Supercomputación, Jordi  
25 Girona, 29, 08034 Barcelona, Spain

26 <sup>12</sup>CIEMAT, Atmospheric Pollution Unit, Avda. Complutense, 22, 28040 Madrid, Spain

27 <sup>13</sup>Faculty of Science and Technology, University of Tromsø, Tromsø, Norway

28 <sup>14</sup>Max-Planck-Institut für Chemie, Mainz, Germany

29 <sup>15</sup>CEREA, Joint Laboratory Ecole des Ponts ParisTech – EDF R&D, Champs-Sur-  
30 Marne, France

31  
32  
33  
34  
35 **Abstract.** The implementation of European emission abatement strategies has led to  
36 significant reduction in the emissions of ozone precursors during the last decade.  
37 Ground level ozone is also influenced by meteorological factors such as temperature,  
38 which exhibit interannual variability, and are expected to change in the future. The  
39 impacts of climate change on air quality are usually investigated through air quality  
40 models that simulate interactions between emissions, meteorology and chemistry.  
41 Within a multi-model assessment, this study aims to better understand how air quality  
42 models represent the relationship between meteorological variables and surface ozone  
43 concentrations over Europe. A multiple linear regression (MLR) approach is applied to  
44 observed and modelled time series across ten European regions in springtime and  
45 summertime for the period of 2000-2010 for both models and observations. Overall, the  
46 air quality models are in better agreement with observations in summertime than in  
47 springtime, and particularly in certain regions, such as France, Mid-Europe or East-  
48 Europe, where local meteorological variables show a strong influence on surface ozone  
49 concentrations. Larger discrepancies are found for the southern regions, such as the

50 Balkans, the Iberian Peninsula and the Mediterranean basin, especially in springtime.  
51 We show that the air quality models do not properly reproduce the sensitivity of surface  
52 ozone to some of the main meteorological drivers, such as maximum temperature,  
53 relative humidity and surface solar radiation. Specifically, all air quality models show  
54 more limitations to capture the strength of the ozone-relative humidity relationship  
55 detected in the observed time series in most of the regions, in both seasons. Here, we  
56 speculate that dry deposition schemes in the air quality models might play an essential  
57 role to capture this relationship. We further quantify the relationship between ozone and  
58 maximum temperature ( $m_{o_3-T}$ , climate penalty) in observations and air quality models.  
59 In summertime, most of the air quality models are able to reproduce reasonably well the  
60 observed climate penalty in certain regions such as France, Mid-Europe and North Italy.  
61 However, larger discrepancies are found in springtime, where air quality models tend to  
62 overestimate the magnitude of observed climate penalty.

## 73 1. Introduction

74  
75 Tropospheric ozone is recognised as a threat to human health and ecosystem  
76 productivity (Mills et al. 2007). It is produced by photochemical oxidation of carbon  
77 monoxide and volatile organic compounds (VOCs) in the presence of nitrogen oxides  
78 ( $NO_x=NO+NO_2$ ) (Jacob and Winner, 2009). While it is an important pollutant on a  
79 regional scale, due to the long-range transport effect it may also influence air quality on  
80 a hemispheric scale (Hedegaard et al, 2013, Monks et al., 2015). Previous studies have  
81 shown that the reduction of emissions of ozone precursors, lead to a decrease in  
82 tropospheric ozone concentrations in Europe (Solberg et al. 2005, Jonson et al. 2006).  
83 However, there is also a large year-to-year variability due to weather conditions  
84 (Andersson et al. 2007).

85  
86 Ozone variability is strongly related to meteorological conditions. Significant  
87 correlations between ozone and temperature have been associated with the temperature-  
88 dependent lifetime of peroxyacetyl nitrate (PAN), and also due to the temperature  
89 dependence of biogenic emission of isoprene (Sillman and Samson, 1995). Substantial  
90 increases in surface ozone have been associated with high temperatures and stable  
91 anticyclonic, sunny conditions that promote ozone formation (Solberg et al. 2008).  
92 Moreover, its strong relationship with temperature represents a major concern, since  
93 under a changing climate the efforts on new air pollution mitigation strategies might be  
94 insufficient. This effect, referred to as the climate penalty (Wu et al., 2008), is expected  
95 to play an important role in future air quality (Hendriks et al. 2016). Similarly,  
96 increasing solar radiation leads to high levels of ozone, though with a weak correlation  
97 (Dawson et al. 2007) and it has been suggested that it could reflect in part the  
98 association of clear sky with high temperatures (Ordóñez et al., 2005). Humidity  
99 influences photochemistry through reactions between water vapor and atomic oxygen

100 (Vautard et al. 2012). High levels of humidity are normally related to enhanced cloud  
101 cover and thus reduced photochemistry (Dueñas et al. 2002, Camalier et al. 2007).The  
102 relationship between ozone and relative humidity can be also explained by dry  
103 deposition through stomatal uptake: under low levels of humidity plants close their  
104 stomata, which reduce the biogenic uptake (Hodnebrog et al. 2012, Kavassalis and  
105 Murphy, 2017). High wind speed is usually correlated with low ozone concentrations  
106 due to enhanced advection and deposition, although the processes involved are complex  
107 and studies from different regions reported weak or insignificant correlations (Dawson  
108 et al., 2007, Jacob and Winner, 2009).

109  
110 Chemistry transport models (CTMs) are one of the most common tools to investigate  
111 the impacts of climate change on air quality (Jacob and Winner, 2009, Colette et al.  
112 2015). Due to assumptions, parametrizations and simplifications of processes, the  
113 models themselves are subject to large uncertainties (Manders et al. 2012), which have  
114 been reflected in some regional differences in the magnitude of surface ozone response  
115 to projected climate change (Andersson and Engardt, 2010). Thus, model biases when  
116 compared to observations still remain a concern, especially in terms of the response of  
117 air quality under future climate (Fiore et al. 2009, Rasmussen et al. 2012). Comparisons  
118 between model outputs and measurements of available observational dataset are  
119 essential to evaluate the models ability to reproduce observations. Discrepancies in the  
120 outputs of CTMs can be due chemical and physical processes, fluxes (emissions,  
121 deposition and boundary fluxes) and meteorological processes (Vautard et al. 2012,  
122 Bessagnet et al. 2016). In particular, quantification and isolation of the effects of  
123 meteorology on ozone is a challenge, due to the complex interrelation between ozone,  
124 meteorology, emissions and chemistry (Solberg et al. 2015). Thus, evaluating air quality  
125 models with respect the meteorological inputs is important given that meteorology  
126 drives numerous chemical processes (Vautard et al. 2012). A number of studies have  
127 evaluated the performance of the meteorological models that drive CTMs by comparing  
128 them with observations of weather parameters relevant for air quality (Smyth et al.,  
129 2006, Vautard et al. 2012, Brunner et al. 2014, Makar et al. 2015, Bessagnet et al.  
130 2016).

131  
132 Capturing observed sensitivities of ozone to meteorological factors is required to assess  
133 the confidence in the models and their ability to reproduce the observed relationships  
134 between pollutants and meteorology and better understand potential impacts under  
135 climate change. However, only a few studies have used model simulations to analyse  
136 ozone sensitivities to meteorological parameters. Davis et al. (2011) evaluated the  
137 performance of the Community Multiscale Air Quality (CMAQ) model to reproduce the  
138 ozone sensitivities to meteorology across Eastern US. Their results showed that the  
139 model underestimated the observed ozone sensitivities to temperature and relative  
140 humidity. Recently, Fix et al. (2017) examined the capability of the NRCM-Chem  
141 model to capture the meteorological sensitivities of high/extreme ozone. Overall, they  
142 found substantial differences between the modelled and the observed sensitivities of  
143 high levels of ozone to meteorological drivers that were not consistent between the three  
144 regions of study. Due to the complex interactions and processes, estimating the ozone  
145 sensitivities to key meteorological variables remains a challenge. Thus, we aim to  
146 examine the capabilities of a set of CTMs to reproduce the observed ozone responses to  
147 meteorological variables. To our knowledge, this is the first multi-model evaluation that  
148 compares observed and modelled meteorological sensitivities of ozone over Europe  
149 using a set of regional air quality models.

150

151 The EURODELTA-Trends (EDT) exercise has been designed to better understand the  
152 evolution of air pollution and assess the efficiency of mitigation strategies for  
153 improving air quality. The EDT exercise allows the evaluation of the skill of regional  
154 air quality models and quantification of the role of the different key driving factors of  
155 surface ozone, such as emissions changes, long-range transport and meteorological  
156 variability (more details on the EDT exercise can be found in Colette et al. 2017a).  
157 Earlier phases of EURODELTA and other relevant modelling exercises, such as  
158 AQMEII (Air Quality Model Evaluation International Initiative, Rao et al. 2009)  
159 covered a short period of time of one year, while only a few studies assessed long-term  
160 air quality but limited to one model (Vautard et al., 2006, Jonson et al. 2006, Wilson et  
161 al. 2012), or utilised climate data rather than reanalysed meteorology (e.g. Simpson et  
162 al., 2014; Colette et al., 2015). The EDT exercise presents a multi-model hindcast of air  
163 quality over 2 decades (1990-2010), and thus offers a good opportunity to evaluate the  
164 role of driving meteorological factors on ozone variability.

165

166 The present study provides a novel and simple method to evaluate the performance of  
167 air quality models in terms of meteorological sensitivities of ozone. Specifically, our  
168 analysis focuses on the European ozone season (April to September) over the years  
169 2000-2010. The choice of this period is mainly motivated by the availability of the  
170 observational dataset from Schnell et al. (2014, 2015) (see section 2.1). Within the EDT  
171 framework, a recent report has presented the main findings on the long-term evolution  
172 of air quality (Colette et al. 2017b). Part of these results was obtained from the analysis  
173 of the 1990s (1990-2000) and 2000s (2000-2010) separately. We focus on the second  
174 decade (2000-2010), for which the interpolated dataset of observed maximum daily 8-  
175 hourly mean ozone (MDA8 O<sub>3</sub>) used in this study was available. Similarly to Otero et  
176 al. (2016), we apply a multiple linear regression approach to examine the  
177 meteorological influence on MDA8 O<sub>3</sub>. Statistical models are developed separately for  
178 observational datasets and air quality models, with the primary focus on examining both  
179 observed and simulated relationships between MDA8 O<sub>3</sub> and meteorological drivers .

180

181 The present paper is structured as follows. Section 2 describes the observational data as  
182 well as the air quality models studied here. The methodology and the design of the  
183 statistical models are introduced in section 3. Section 4 discusses the results and the  
184 summary and conclusions are discussed in section 5.

185

## 186 2. Data

187

### 188 2.1. Observations

189

190 This study uses gridded MDA8 O<sub>3</sub> concentrations created with an objective-mapping  
191 algorithm developed by Schnell et al. (2014). They applied a new interpolation  
192 technique over hourly observations of stations from the European Monitoring and  
193 Evaluation Programme (EMEP) and the European Environment Agency's air quality  
194 database (AirBase) to calculate surface ozone averaged over 1° by 1° grid cells (see  
195 Schnell et al., 2014, 2015). Otero et al. (2016) used this dataset for examining the  
196 influence of synoptic and local meteorological conditions over Europe. This  
197 interpolated product offers a possibility to establish a direct comparison between  
198 observations and CTMs. However, it must be acknowledged that for some areas with a  
199 low number of stations (i.e. the southeastern or northeastern European regions) the

200 values interpolated into the 1°x1° degree grid cells may not be representative of such  
201 large scales. Recently, Ordóñez et al. (2017) and Carro-Calvo et al. (2017) have used  
202 this product to assess the impact of high-latitude and subtropical anticyclonic systems  
203 on surface ozone and the synoptic drivers of summer ozone respectively. They reported  
204 inhomogeneities during some years for specific grid-cells (e.g. in the Balkans and  
205 Sweden), which were excluded from their analysis. However, we did not observe a clear  
206 shift when analysing the spatial averages of the time series of the MDA8 O<sub>3</sub> for those  
207 particular regions (e.g. Balkans and Scandinavia) (Figs. S1, S2), Therefore our analysis  
208 includes the whole dataset.

209

210 This study investigates the influence of observed meteorological variables on MDA8  
211 O<sub>3</sub>, based on the ERA-Interim reanalysis product provided by the European Centre for  
212 Medium-Range Weather Forecasts (ECMWF) at 1°x1° resolution (Dee et al. 2011).  
213 Meteorological reanalyses products are essentially model simulations constrained by  
214 observations and they have been widely validated against independent observations.  
215 Daily mean values are calculated as the mean of the four available time steps at 00, 06,  
216 12, and 18UTC for 10m wind speed components (u and v) and 2m relative humidity.  
217 Maximum temperature is approximated by the daily maximum of those time steps,  
218 while daily mean surface solar radiation is obtained from the 3-hourly values provided  
219 for the forecast fields.

220

## 221 2.2. Chemistry Transport Models (CTMs)

222

223 A set of state-of-the-art air quality models participating in the EDT exercise is used  
224 here: LOTOS-EUROS (Schaap et al., 2008, Manders et al. 2017), EMEP/MSC-W  
225 (Simpson et al., 2012), CHIMERE (Mailer et al., 2017), MATCH (Robertson et al.,  
226 1999) and MINNI (Mircea et al., 2016). The domain of the CTMs extends from 17°W  
227 to 39.8°E and from 32°N to 70°N and it follows a regular latitude-longitude projection  
228 of 0.25x0.4 respectively. The main features of the CTM setup are largely constrained by  
229 the EDT experimental protocol (e.g. meteorology, boundary conditions, emissions,  
230 resolution, see Colette et al. 2017a for further details). For instance, the boundary  
231 conditions were defined from a climatology of observational data for most of the  
232 experiments of the EDT exercise (including the data used here). However, the  
233 representation of physical and chemical processes and the vertical distribution differ in  
234 the CTMs, as well as the vertical distribution of model layers (including altitude of the  
235 top layer and derivation of surface concentration at 3m height in the case of EMEP,  
236 LOTOS-EUROS and MATCH). Moreover, there were no specific constrains imposed  
237 on biogenic emissions (including soil NO emissions), which are represented by most of  
238 the models using an online module (Colette et al. 2017a). Since we aim here to  
239 compare the modelled relationship between meteorology and surface ozone, prescribing  
240 common features in the CTMs is particularly an advantage to identify potential sources  
241 of discrepancies.

242

243 The CTMs were forced by regional numerical weather model simulations using  
244 boundary conditions from the ERA-Interim global reanalysis (Dee et al., 2011). Most of  
245 the CTMs used the same meteorological input data, with a few exceptions. Three of  
246 them (EMEP, CHIMERE and MINNI) used input meteorology from the Weather  
247 Research and Forecast Model (WRF) (Skamarock et al. 2008). LOTOS-EUROS and  
248 MATCH used the input meteorology produced by RACMO2 (van Meijgaard, 2012) and  
249 HIRLAM (Dahlgren et al. 2016), respectively. Unlike the rest of the regional weather

250 models, RACMO2 used in the EDT exercise excluded nudging towards ERA-Interim,  
251 which might have some impact in the meteorological fields generated by RACMO2. A  
252 summary of the CTMs and the corresponding sources of meteorological input data with  
253 some of the main characteristics are given in Table 1. As with the observations, CTMs  
254 and their meteorological counterpart were interpolated to a common grid with  $1^\circ \times 1^\circ$   
255 horizontal resolution. The use of a coarser resolution could have an impact in some  
256 regions with a complex orography where airflow is usually controlled by mesoscale  
257 phenomena (e.g. see-breeze and mountain-valley winds) or in regions characterized by  
258 high emission densities (Schaap et al., 2015, Gan et al. 2016). In such cases the use of a  
259 finer grid could be beneficial to capture the variability of local processes.

260  
261 A set of meteorological parameters was selected from the meteorological input data for  
262 the regression analyses. Similarly to the procedure with ERA-Interim, daily means are  
263 obtained from the available time steps every 3 hours in the case of WRF and RACMO2,  
264 and every 6 hours for HIRLAM for the following variables: 10m wind speed  
265 components, 2m relative humidity and surface solar radiation. Maximum temperature is  
266 also approximated by the daily maximum of those time steps.

### 267 268 **3. Multiple linear regression model**

269  
270 Summertime usually brings favourable conditions for high near-surface ozone  
271 concentrations, such as air stagnation due to high-pressure systems, warmer  
272 temperatures, higher UV radiation, and lower cloud cover (Dawson et al. 2007). This  
273 study attempts to better understand how CTMs represent the meteorological sensitivities  
274 of ozone. To this aim, we use a multiple linear regression approach that can provide  
275 useful information of sensitivities in the distribution of ozone concentration as a whole  
276 (Porter et al., 2015).

277  
278 A total of five meteorological predictors (Table 2) are selected based on the existing  
279 literature that has shown their strong influence on ozone pollution (e.g. Bloomfield et al.  
280 1996, Barrero et al. 2005, Camalier et al. 2007, Dawson et al. 2007, Andersson and  
281 Engardt, 2010, Rasmussen et al. 2012, Davis et al. 2011, Doherty et al., 2013, Otero et  
282 al. 2016). Moreover, it has been shown that the occurrence of air pollution episodes  
283 might increase when the pollution levels of the previous day are higher than normal  
284 (Ziomas et al. 1995). Then, apart from the meteorological predictors, we add the effect  
285 of the lag of ozone (MDA8 from the previous day) in order to examine the role of ozone  
286 persistence. Additionally, we include harmonic functions that capture the effect of  
287 seasonality as in Rust et al. al (2009) and Otero et al. (2016), which is referred as “day”  
288 in the MLRs (see Table 2).

289  
290 For this study, we divide the European domain into 10 regions: England (EN), Inflow  
291 (IN), Iberian Peninsula (IP), France (FR), Mid-Europe (ME), Scandinavia (SC), North  
292 Italy (NI), Mediterranean (MD), Balkans (BA) and Eastern Europe (EA). These regions  
293 are based on those defined in the recent ETC/ACM Technical Paper (Colette et al.  
294 2017b). For our study, we further subdivide the original Mediterranean region (MD)  
295 into a region covering the Balkans (BA), due to the strong influence of the ozone  
296 persistence on MDA8 O<sub>3</sub> over this particular region as noted previously in Otero et al.  
297 (2016). Figure 1 shows the spatial coverage of each region and Table 3 lists their  
298 coordinates. As shown in Otero et al. (2016), the relative importance of predictors in the  
299 MLRs shows distinct seasonal patterns. Here, multiple linear regression models (MLR,

300 hereafter) are developed for each region for two seasons: springtime (April-May-June,  
 301 AMJ) and summertime (July-August-September, JAS). These seasons differ from the  
 302 meteorological definition, but cover the period when surface ozone typically reaches its  
 303 highest concentrations (i.e. April-September). Additionally, we analysed the impact of  
 304 the seasons' definition by performing sensitivity tests using the meteorological seasons  
 305 (i.e. March-May-April, MAM and June-July-August, JJA). As shown in Figs. S3 and S4  
 306 (see Supplement), we found a stronger impact of some relevant key driving factors of  
 307 ozone (e.g. temperature and relative humidity) when using the seasons defined above  
 308 (AMJ and JAS) than when using the meteorological seasons. Therefore, we consider  
 309 that our choice of 3-month periods that cover the whole ozone season is particularly  
 310 useful for examining the impact of individual meteorological parameters when ozone  
 311 levels are highest. Since the domains covered by observations and CTMs do not  
 312 coincide exactly, we applied an observational-mask to use the same number of grid-  
 313 cells for CTMs and observations. Data used to estimate parameters of the MLR were  
 314 spatially averaged over each region. Thus, we compare MLRs developed separately for  
 315 CTMs and observations for each region and season. The observational dataset contains  
 316 the gridded MDA8 O<sub>3</sub> and the meteorology input from ERA-Interim, while the dataset  
 317 for the CTMs contains the MDA8 O<sub>3</sub> from each one of them along with the  
 318 corresponding meteorological input (LOTOS and RACMO2, CHIMERE and WRF,  
 319 MATCH and HIRLAM) (see Table 1).

320

321 A MLR is built to describe the relationship between MDA8 O<sub>3</sub> (predictand) and a set of  
 322 covariates (or predictors) describing seasonality, ozone persistence and the influence of  
 323 meteorological fields (Table 2). A data series  $y_t$ ,  $t = 1, \dots, N$  (e.g. observations or CTM  
 324 simulations) for a given region and season is conceived as a Gaussian random variable  
 325  $Y_t$  with varying mean  $\mu_t$  and homogeneous variance  $\sigma^2$ . The mean  $\mu_t$  is described as a  
 326 linear function of the covariates, i.e.

327

$$328 Y_t \sim \mathcal{N}(\mu_t, \sigma^2),$$

$$329 \mu_t = \beta_0 + \beta_{sin} \sin\left(\frac{2\pi}{365.25} d_t\right) + \beta_{cos} \cos\left(\frac{2\pi}{365.25} d_t\right) + \beta_{lag} y_{t-1} + \sum_{k=1}^K \beta_k x_{t,k} \quad (1)$$

330

331 with  $t$  indexing daily values and  $d_t$  referring to the day in the year associated with the  
 332 index  $t$ .  $\beta_0$  is a constant offset,  $\beta_{sin}$  and  $\beta_{cos}$  are the first order coefficient of a Fourier  
 333 series (e.g. Rust et al. 2009, 2013, Fischer et al. 2017),  $\beta_{lag}$  describes the persistence  
 334 with respect to the previous day concentration  $y_{t-1}$ ; if  $t$  is the first day in the late  
 335 summer season (JAS, July 1<sup>st</sup>),  $y_{t-1}$  is the concentration of June 30<sup>th</sup>. Further regression  
 336 coefficients  $\beta_k$  describe the linear relation to potential meteorological drivers (see table  
 337 2). For covariates standardized to unit variance, the regression coefficients ( $\beta$ ) are  
 338 standardised coefficients giving the change in the predictand with the covariate in units  
 339 of covariate standard deviation.

340

341 Following the same strategy as used in Otero et al. (2016), the MLRs are developed  
 342 through several common steps: 1) starting with the full set of potentially useful  
 343 components in the predictor, a stepwise backward regression using the Akaike  
 344 Information Criterion (AIC) as a selection criterion removes successively those  
 345 components in the predictor, which contribute least to the model performance; and 2) a  
 346 multi-collinearity index known as variance inflation factor (VIF, Maindonald and Braun  
 347 2006) is used to detect multi-collinearity problems in the predictor (i.e. high correlations

348 between two or more components in the predictor). Components with a VIF above 10  
349 are left out of the predictor (Kutner et al 2004).

350

351 The statistical performance of each MLR (built separately from observations and  
352 CTMs) is assessed through the adjusted coefficient ( $R^2$ ) and the root mean square error  
353 (RMSE). The  $R^2$  estimates the fraction of total variability described by the MLR and the  
354 RMSE gives the average deviation between model and observation obtained in the  
355 MLR. We also examine the relative importance of the individual components in the  
356 predictor. According to the method proposed by Lindeman et al (1980), the relative  
357 importance of each predictor is estimated by its contribution to the  $R^2$  coefficient  
358 (Grömping 2007). We assess the sensitivities of ozone to the predictors through the  
359 standardised coefficients obtained from the regression. These coefficients indicate the  
360 changes in the ozone response to the changes in the predictors, in terms of standard  
361 deviation. Thus, for every standard deviation unit increase (decrease) of a specific  
362 predictor, the predictand (MDA8 O<sub>3</sub>) will increase (decrease) the amount indicated by  
363 its coefficient in standard deviation units,. The use of standardised coefficients allows  
364 us to establish a direct comparison in the influence of individual predictors. The effect  
365 of seasonality introduced by the harmonic functions (namely, “day”, table 2) is kept in  
366 the MLRs (Eq. 1) for its usefulness in improving the power of the regression analysis,  
367 however further explanation about the effect of the predictors focuses on the rest of the  
368 variables.

369

## 370 4. Results and discussion

371

### 372 4.1. CTM performance by region

373

374 We compare the seasonal cycle of observations and CTM results through the time series  
375 of daily averaged values of MDA8 O<sub>3</sub> from observations and CTMs for the whole  
376 period (i.e. April-September, 2000-2010) spatially averaged over each region.  
377 Furthermore, correlation coefficients between both CTMs and observations at each  
378 region and season are used to quantify the CTM performance.

379

#### 380 4.1.1. Seasonal cycle of MDA8 O<sub>3</sub>

381

382 We examine the ozone seasonal cycle represented by both the observational and  
383 modelled dataset. Figure 2 depicts daily averages during 2000-2010 of MDA8 O<sub>3</sub> at  
384 each region for the CTMs and observations. In general, all CTMs are biased high  
385 compared with observations. CTM results are visually closer to observations in the  
386 northwestern regions (i.e. IN, EN and FR), while the spread becomes larger over the  
387 southern and southeastern regions (i.e. BA, NI, MD). The IN, EN and SC regions show  
388 the highest observed concentrations in the starting months (AMJ), which is not  
389 generally well captured by most of the CTMs, which show a more flat timeline (e.g.  
390 LOTOS, MATCH, CHIMERE). For example, in the SC region, some of the CTMs  
391 underestimate the ozone concentrations in AMJ (i.e. CHIMERE and MINNI). The rest  
392 of the regions show the highest observed concentrations in JAS, which is generally  
393 overestimated by the CTMs. Models show discrepancies in the ozone seasonal cycle  
394 when compared to each other and when compared against observations. For example,  
395 we observed substantial differences in the southern regions, such as IP, MD and BA,  
396 where the models show a considerable spread. In those regions, the CTMs exhibit a  
397 different behaviour when compared to each other. For instance, the EMEP model shows



398 ozone peak concentrations in April, while CHIMERE and MINNI show a peak in July.  
399 Overall LOTOS shows a relatively constant positive bias in all regions, more evident in  
400 the MD and NI regions.

401

402

403

#### 4.1.2. Correlation coefficients between modelled and observed time series

404

405 The correlation coefficients between the observed and modelled values of MDA8 O<sub>3</sub> at  
406 each region and in each season are shown in Fig. 3. Overall, MDA8 O<sub>3</sub> from the CTMs  
407 is better correlated with observations in JAS than in AMJ in the regions ME, NI, EA  
408 and EN. As expected from inspection of the average time series (Fig. 2), the lowest  
409 correlations between models and observations are found in BA, especially in AMJ for  
410 all models. In particular, EMEP is negatively correlated with observations over this  
411 region. As mentioned above, the larger discrepancies between CTMs and observations  
412 found over BA might be attributed to a low density of observation sites from which the  
413 interpolated dataset is derived, resulting in a lower quality or higher uncertainties of  
414 such products (Schnell et al. 2014). The highest correlations in AMJ are obtained at the  
415 following regions: ME; FR; NI; and EN for most of the models, except for EMEP for  
416 which the highest correlation with observations was found in IN and SC. In general, the  
417 models that are most closely correlated with observations are MATCH, MINNI and  
418 CHIMERE, while LOTOS shows the lowest correlations, which could be partially due  
419 to the use of a different set-up of the RACMO2 model, without nudging towards ERA-  
420 Interim (section 2.2). These correlations reflect the patterns represented by the seasonal  
421 cycle described above.

422

423

#### 4.2. MLR performance

424

425 Figures 4 and 5 depict the statistical performance of each MLR in terms of R<sup>2</sup> and  
426 RMSE (respectively) at the different regions for both seasons, AMJ and JAS. The R<sup>2</sup>  
427 values indicate that all MLRs models (based on both observations and CTMs) are able  
428 to explain more than 60% of the MDA8 O<sub>3</sub> variance in all regions. Overall, the MLRs  
429 show a stronger fit in JAS than in AMJ in most of the regions (Fig. 4). The MLRs  
430 appear to perform better in regions such as NI, ME, FR or EA, while the poorest  
431 statistical performance is found in IN and EN. The results obtained from the CTM-  
432 based MLRs show a similar performance to the observation-based MLRs in most of the  
433 regions. The lowest RMSE values for most of the MLR are found in SC ranging  
434 between 1 and 3 ppb, while EN shows the largest RMSE values. The MLRs from  
435 MATCH and CHIMERE show the lowest RMSE values (1-3ppb) suggesting the best  
436 statistical fit from a predictive point of view.

437

438 Both R<sup>2</sup> and RMSE metrics indicate that the statistical performance of MLRs for  
439 observations and CTMs show distinct variations between seasons and regions. Overall,  
440 better performances are found in JAS and in some regions (i.e. ME, NI, or FR) where  
441 MLRs are able to describe more than the 80% of the variance in CTMs and  
442 observations. This could be attributed to the major role of meteorology in summer  
443 influencing local photochemistry processes of ozone production, while in spring long  
444 range transport plays a stronger role (Monks, 2000, Tarasova et al. 2007). As it includes  
445 the bias, the RMSE reveals more differences among the MLRs when compared to each  
446 other (e.g. larger errors for LOTOS when compared to MATCH or CHIMERE).  
447 However, it is interesting that in general all MLRs show a similar tendency when

448 evaluating the statistical performance, which indicate that observations-based and  
449 CTMs-based MLRs present a similar statistical performance for modelling MDA8 O<sub>3</sub>.  
450 The ability of the CTMs to reproduce the influence of meteorological drivers on MDA8  
451 O<sub>3</sub> is discussed in more detail below.

452

### 453 **4.3. Effects of drivers on ozone concentrations**

454

455 The analysis of the influence of the predictors in the MLRs reveals distinctive regional  
456 patterns in both observation-based and CTM-based MLRs. In agreement with Otero et  
457 al. (2016), here we also find that the regions geographically located towards the interior  
458 (including central, western and eastern regions) appear to be more sensitive to the  
459 meteorological predictors, especially in JAS. On the contrary, less meteorological  
460 contribution is found in the regions over the northernmost and southernmost part of the  
461 domain, implying that non-local processes (e.g. long-range transport) play a stronger  
462 role here. Considering such similarities, in the following, the regions: EN, FR, ME, NI  
463 and EA are referred as the internal regions, while the rest of the regions: IN, SC, IP, MD  
464 and BA, are referred as the external regions (see Fig. 1).

465

#### 466 4.3.1 Relative importance

467

468 Figure 6 depicts the relative importance of the predictors for the observation-based and  
469 CTM-based MLRs in the internal regions (Fig. 1). Here, a larger meteorological  
470 influence (i.e., the predictors other than LO<sub>3</sub> and day) can be seen in JAS compared to  
471 AMJ in all of these regions. In general, the dominant meteorological drivers from the  
472 observation-based MLRs in these internal regions are RH and Tx. The contribution of  
473 RH is evident in AMJ (e.g. ME, or EA), while Tx is clearly dominant in JAS. SSRD is  
474 also a key driver of MDA8 O<sub>3</sub> and generally, the wind factors (W10m and Wdir) appear  
475 to have a minor contribution.

476

477 Despite the CTM-based MLRs being able to capture the meteorological predictors, we  
478 observe discrepancies among the internal regions when compared to the observation-  
479 based MLR. The inter-model differences in terms of the relative importance of  
480 predictors are greater in AMJ than in JAS. For instance, the contribution of the LO<sub>3</sub> is  
481 overestimated by most of CTMs. Substantial differences are found in the influence of  
482 RH when comparing the observation-based and the CTMs-based models. The CTMs do  
483 not capture the relative importance of the RH well, especially in AMJ. In general, the  
484 CTMs driven by WRF meteorology show a slightly larger contribution of RH in most of  
485 the cases, although we notice that there are also some differences among the models that  
486 share the same meteorology. CTMs do capture the relative importance of Tx in all  
487 regions, but overall they overestimate it, as they also show for SSRD. Here, we find  
488 discrepancies when comparing the contribution of predictors in the statistical models  
489 from CTMs driven by the same meteorology (e.g. EMEP when compared to CHIMERE  
490 and MINNI). Such differences among the models using the same meteorology point out  
491 that the model setup (e.g. number of vertical levels, depth of first layer) and model  
492 parameterizations (e.g. chemistry/physical processes) have a larger influence in the  
493 model performance than the meteorological processes.

494

495 Figure 7 presents the relative importance of individual predictors in the MLRs  
496 developed at the external regions (Fig. 1) for both seasons. The observation-based  
497 MLRs show that the main driving factor is LO<sub>3</sub> in AMJ, while the effect of

498 meteorological drivers becomes stronger in JAS. RH presents a larger contribution in  
499 some regions (e.g. IN, IP or SC) in AMJ and Tx in JAS (e.g. IN, IP, SC and BA). The  
500 contribution of wind components, Wdir and W10m, is mainly reflected in both seasons  
501 in the western regions (i.e. IN and IP) and in MD, respectively.

502  
503 Overall, all CTMs show this tendency, although there are substantial differences when  
504 comparing the individual drivers' contribution in the observation-based and CTM-based  
505 MLRs, particularly in AMJ (Fig. 7). CTMs do not capture the contribution of LO3  
506 reflected by the observation-based MLRs. As in the previous analysis (section 4.1) the  
507 largest discrepancies are found in BA. In this region, the observation-based MLR shows  
508 that most of the variability of ozone would be explained by LO3, while the CTM-based  
509 MLRs underestimate the contribution of LO3 and overestimate the meteorological  
510 contribution of Tx, SSRD and RH (e.g. LOTOS, CHIMERE and MINNI). The  
511 contribution of RH is, again, underestimated by the CTMs in most of the regions,  
512 (except in BA). On the contrary, the relative importance of SSRD is overestimated in  
513 some regions (e.g. IP, IN or MD) and Tx (IN, SC), in particular for the CTMs driven by  
514 WRF. Overall, CTMs show the observed contribution of W10m and Wdir in both  
515 seasons, although with some inconsistencies among the regions and CTMs.

516  
517 Our results indicate that the relative importance of meteorological factors is stronger in  
518 the internal regions (Fig.6) than in the external regions (Fig.7), which could be partially  
519 attributed to a larger variability of most of the meteorological fields in internal regions  
520 (Fig. S5). The external regions are also more likely to be influenced by the lateral  
521 boundary conditions applied by each CTM. In addition, in some external regions (e.g.  
522 IP or MD), as mentioned in section 2, the use of a coarser grid in some regions might be  
523 insufficient to capture mesoscale processes, such as land-sea breezes, which also control  
524 MDA8 O<sub>3</sub> concentrations (Millán et al. 2002). Moreover, we observe that meteorology  
525 becomes more important in summer, when local photochemistry processes are  
526 dominant. In general, CTMs show this tendency, but limitations to reproduce the effect  
527 of some meteorological drivers are found. Specifically, while CTMs tend to  
528 overestimate the contribution of Tx, and SSRD, they underestimate the relative  
529 importance of RH, which is also reflected in the correlations coefficients between  
530 predictand the predictors (Figs. S6, S7).

531

#### 532 4.3.2 Sensitivity of ozone to the drivers

533

534 We assess the sensitivities of MDA8 O<sub>3</sub> to the drivers through their standardised  
535 coefficients obtained in the MLR (Section 3). These coefficients provide further  
536 information about the changes of MDA8 O<sub>3</sub> due to the effect of each driver. Figures 8  
537 and 9 depict the values of the main driving factors obtained in the MLR for the internal  
538 and the external regions (respectively): LO3, Tx and RH. Similarly to those patterns  
539 described by the relative importance of drivers, we observe that the ozone response to  
540 LO3 is stronger in AMJ than in JAS: the corresponding standardised coefficients are  
541 always positive and generally higher in AMJ. The observed sensitivities to LO3 are  
542 smaller in the internal regions (Fig. 8), being particularly dominant in the external  
543 regions (Fig. 9). Overall, most of the CTMs reflect a similar tendency. However, there  
544 are evident differences between observations and CTMs when comparing the values of  
545 the standardised coefficients, specifically in some regions such as BA or MD. When  
546 comparing the ozone responses of the CTMs to LO3, we observe that in most of the

547 regions MATCH and MINNI show values closest to observations, which is consistent  
548 with the results described at the beginning of this section (4.1.2).

549

550 Correlations between MDA8 O<sub>3</sub> and Tx are strong, especially in the internal regions in  
551 JAS (Fig. S6). Overall, we show that the CTMs appear to capture the observed effect of  
552 Tx better in JAS than in AMJ in most of the regions. The highest sensitivities to Tx are  
553 found in internal regions such as ME, NI, FR and EN, which is also shown in the CTMs  
554 (Fig. 8). However, we see that most of the CTMs tend to overestimate the effect of Tx  
555 and distinct sensitivities to Tx are also found for those models that share the same  
556 meteorology (i.e. CHIMERE, EMEP and MINNI). In particular, the MINNI and  
557 CHIMERE models show higher Tx sensitivities when compared to the rest of the  
558 CTMs. While the MINNI model presents the highest sensitivities to Tx in spring,  
559 especially in EN and FR, EMEP shows smaller values and it underestimates the  
560 correlations between Tx and MDA8 O<sub>3</sub> (Figs. S6, S7).

561

562 The slope of the ozone-temperature relationship ( $m_{O_3-T}$ ) has been used in several studies  
563 to assess the ozone climate penalty (eg. Bloomer et al., 2009, Steiner et al., 2010,  
564 Rasmussen et al., 2012, Brown-Steiner et al. 2015) in the context of future air quality.  
565 Thus, we additionally analyse the ozone-temperature relationship in order to provide  
566 insight into the ability of CTMs to reproduce the observed  $m_{O_3-T}$ . Similarly to previous  
567 work (Brown-Steiner et al. 2015), the slopes are obtained from a simple linear  
568 regression using only Tx (without the influence from other predictors) and they are used  
569 to quantify such relationship in both seasons, AMJ and JAS.

570

571 Figures 10 and 11 illustrate the  $m_{O_3-T}$  for the internal and the external regions  
572 respectively. The observed  $m_{O_3-T}$  is larger in JAS than in AMJ. In AMJ, it ranges  
573 between -0.45 and 1.15 ppbK<sup>-1</sup> with the largest values found in ME, NI and MD. In  
574 JAS, the observed climate penalty is of the order of 1-2.7 ppbK<sup>-1</sup> with the largest values  
575 in EN, FR, ME, NI, and MD. CTMs show a better agreement with observations in JAS  
576 than in AMJ. CTMs tend to overestimate the climate penalty in AMJ in most of the  
577 regions, with some exceptions, such as EMEP and MATCH that systematically  
578 underestimate the slopes. Also, CTMs are generally better in simulating the observed  
579  $m_{O_3-T}$  in the internal regions compared to the  $m_{O_3-T}$  in the external regions, where in  
580 general CTMs appear to overestimate the climate penalty in both seasons. Using this  
581 metric, we identify some regions particularly sensitive to temperature, with larger  
582 values of  $m_{O_3-T}$  (e.g. EN, ME, FR, NI or MD). Through a multi-model assessment,  
583 Colette et al. (2015) showed a significant summertime climate penalty in southern,  
584 western and central European regions (e.g. EA, IP, FR, ME or MD) in the majority of  
585 the future climate scenarios used. Our study shows that most of the CTMs confirm the  
586 observed climate penalty in JAS in such regions in the near present, although we found  
587 that most of the CTMs overestimate the climate penalty in AMJ, especially in the  
588 external regions.

589

590 We see a stronger effect of RH in AMJ than in JAS in the observations with the greatest  
591 impact in the internal regions (e.g. EA, ME, NI, FR and EN), which is not well  
592 represented by the CTMs (Figs. 8 and 9). As mentioned, CTMs underestimate the  
593 strength of the correlations between ozone and relative humidity (Figs. S6, S7). This  
594 general lack of sensitivity to RH could also partially explain the tendency for all CTMs  
595 to show a high bias in simulated ozone compared with observations (Fig. 2). Among  
596 the possible reasons for this inconsistency, we hypothesize that it can be related to the

597 fact that ozone removal processes can be associated with higher relative humidity levels  
598 during thunderstorm activity on hot moist days, which might not be well captured by  
599 CTMs. As previous studies pointed out (e.g. Andersson and Engardt, 2010), the impacts  
600 of ozone dry deposition suggest that it may also play a role in explaining the problems  
601 that CTMs show to reproduce the observed ozone-relative humidity relationship. With a  
602 simple modelling approach, Kavassalis and Murphy (2017) found that the relationship  
603 between ozone and relative humidity was better captured by the inclusion of the vapour  
604 pressure deficit-dependent dry deposition, pointing out the relevance of detailed dry  
605 deposition schemes in the CTMs.

606  
607 High SSRD levels favour photochemical ozone formation and it is usually positively  
608 correlated to ozone. In this case, CTMs also present some limitations to capture this  
609 effect and they overestimated the sensitivities of ozone to SSRD (Figs. S8, S9). For  
610 example, the observations show a lower and surprisingly negative effect of SSRD.  
611 Although the correlations between SSRD and ozone are positive (see Figs. S6, S7), the  
612 presence of other predictors in the regression may reverse the sign of the estimated  
613 coefficient. The CTMs show a stronger sensitivity of ozone to SSRD and they  
614 overestimate its influence on surface ozone. Similarly, the sensitivities to Wdir and  
615 W10m are also overestimated by the CTMs, especially in AMJ (Figs. S8, S9).

616  
617 Our analysis suggests that CTMs present more limitations to reproduce the influence of  
618 meteorological drivers to MDA8 O<sub>3</sub> concentrations in the external regions than in the  
619 internal regions, particularly in AMJ. Moreover, we find the largest discrepancies in  
620 BA, where models show the poorest seasonal performance and correlation coefficients  
621 (Figs. 2 and 3, respectively), probably due a low quality of the observational dataset.

622  
623 Furthermore, LO3 is the main driver over most of the external regions and explains a  
624 large proportion to the total variability of MDA8 O<sub>3</sub>, while meteorological factors play  
625 a smaller influence. Lemaire et al. (2016) found a very low performance (based on R<sup>2</sup>)  
626 over the British Isles, Scandinavia and the Mediterranean using a different statistical  
627 approach that only included two meteorological drivers. They attributed this low skill to  
628 the large influence over those regions of long-range transport of air pollution (Lemaire  
629 et al. 2016). Our results confirm the small influence of the meteorological drivers over  
630 those regions and the strong influence of the ozone persistence. Moreover, in the case of  
631 the external regions of northern Europe, it could also be explained due to the dominance  
632 of transport processes such as the stratospheric-tropospheric exchange or long-range  
633 transport from the European continent, rather than local meteorology, particularly in  
634 AMJ (Monks, 2000, Tang et al. 2009, Andersson et al. 2009).

635  
636 Previous work suggested that local sources of NO<sub>x</sub> and biogenic VOC (ozone  
637 precursors) are important factors of summertime ozone pollution in the Mediterranean  
638 basin (Richards et al. 2013). Moreover, some studies suggested that the local vertical  
639 recirculation and accumulation of pollutants play an important role in ozone pollution  
640 episodes in this region: during the nighttime the air masses are held offshore by land-sea  
641 breeze, creating reservoirs of pollutants that are brought back the following day (Millán  
642 et al. 20002, Jiménez et al. 2006, Querol et al. 2017). All of these factors (e.g. local  
643 emissions as well as local and large-scale processes) control the ozone variability,  
644 which might explain the smaller influence of local meteorological factors shown in this  
645 study over the Mediterranean basin when compared to meteorological influence in the  
646 internal regions. Thus, we may hypothesize that the strong impact of LO3 observed in

647 the external regions over southern Europe (i.e. IP, MD, BA) could be partially due to  
648 the role of vertical accumulation and recirculation of air masses along the  
649 Mediterranean coasts as a result of the mesoscale phenomena, which is enhanced by the  
650 complex terrains that surround the Basin. Other important factor for the strong impact  
651 of LO3 observed is the slow dry deposition of ozone on water that would favour the  
652 ozone persistence in southern Europe.

653

654 Overall we conclude that CTMs capture the effect of meteorological drivers better in the  
655 internal regions (EN, FR, ME, NI and EA), where the influence of local meteorological  
656 conditions is stronger. The major effect of meteorological parameters found in the  
657 internal European regions might be also attributed to the fact that overall the variability  
658 of meteorological conditions is larger in those regions (Fig. S5). We also find  
659 differences among the CTMs driven by the same meteorology. As mentioned in the  
660 introduction, Bessagnet et al. (2016) suggested that the spread in the model results  
661 could be partly explained by the differences in the vertical turbulent mixing in the  
662 planetary boundary layer, differently diagnosed in each of the CTMs. Our results also  
663 indicate that even though models share the same meteorology (considering the  
664 prescribed requirements defined by the EDT exercise) they show discrepancies when  
665 compared to each other, which could be attributed to other sources of uncertainties  
666 (such as physical and chemical internal processes in the CTMs). The NMVOC and NO<sub>x</sub>  
667 emissions from the biosphere are critical in the ozone formation. Since biogenic  
668 emissions were not specifically prescribed, which have a strong dependence on  
669 temperature and solar radiation, discrepancies in the CTMs performances, (e.g. different  
670 sensitivities to Tx) might be expected. Furthermore, we notice that the CTMs do not  
671 reproduce consistently the regional ozone-temperature relationship, which is a key  
672 factor when assessing the impacts of climate change on future air quality.

673

## 674 **5. Summary and conclusions**

675

676 The present study evaluates the capabilities of a set of Chemical Transport Models  
677 (CTMs) to capture the observed meteorological sensitivities of daily maximum 8-hour  
678 average ozone (MDA8 O<sub>3</sub>) over Europe. Our study reveals systematic differences  
679 between the CTMs in reproducing the seasonal cycle when compared to observations.  
680 In general, CTMs tend to overestimate the MDA8 O<sub>3</sub> in most of the regions. In the  
681 western and northern regions (i.e. Inflow, England and Scandinavia), some models did  
682 not capture the high ozone levels in spring (e.g. CHIMERE and MINNI), while in some  
683 southern regions (e.g. Iberian Peninsula, Mediterranean and Balkans) they  
684 overestimated the ozone levels in summer (e.g. LOTOS, CHIMERE). Of the CTMs,  
685 MATCH and MINNI were the most successful in capturing the observed seasonal cycle  
686 of ozone in most regions. All CTMs revealed limitations to reproduce the variability of  
687 ozone over the Balkans region, with a general overestimation of the ozone  
688 concentrations, considerably larger during the warmer months (July, August). As  
689 reflected in the results, a limitation of the interpolated observational product used here  
690 is that in some regions (e.g. southern Europe) it has a lower quality due to a reduced  
691 number of stations (section 2.1).

692

693 The MLRs performed similarly for most of the CTMs and observations, describing  
694 more than 60 % of the total variance of MDA8 O<sub>3</sub>. Overall, the MLRs perform better in  
695 JAS than in AMJ, and the highest percentages of described variance were found in Mid  
696 Europe and North Italy. This could be attributed to local photochemical processes being

697 more important in JAS, and is consistent with a relatively stronger influence of long-  
698 range transport in AMJ.

699

700 The effects of predictors revealed spatial and seasonal patterns, in terms of their relative  
701 importance in the MLRs. Particularly, we noticed a larger local meteorological  
702 influence in the regions located towards the interior of Europe, here termed as the  
703 internal regions (i.e. England, France, Mid-Europe, North Italy and East-Europe). A  
704 minor local meteorological contribution was found in the remaining regions, referred as  
705 the external regions (i.e. Inflow, Iberian Peninsula, Scandinavia, Mediterranean and  
706 Balkans). The CTMs are in better agreement with the observations in the internal  
707 regions than in the external regions, where they were not as successful in reproducing  
708 the effects of the ozone drivers. Overall, the different behaviour in the MLRs developed  
709 in the external regions could be attributed to (i) a larger influence of dynamical  
710 processes rather than local meteorological processes (e.g. long range transport in the  
711 northern regions) (ii) a stronger impact of the boundary conditions (iii) the use of a  
712 coarser grid that might be insufficient to capture mesoscale processes that also influence  
713 MDA8 O<sub>3</sub> (e.g. sea-land breezes in the southern regions).

714

715 We found substantial differences in the sensitivities of MDA8 O<sub>3</sub> to the different  
716 meteorological factors among the CTMs, even when they used the same meteorology.  
717 As Bessagnet et al. (2016) point out, the differences amongst CTMs could be partly  
718 attributed to some other diagnosed model variables (e.g. vertical turbulent mixing and  
719 boundary layer height, as well as vertical model resolution). To assess the effect of such  
720 potential sources of uncertainties, further investigations would be required. Moreover,  
721 variations in the sensitivity of ozone to meteorological parameters could depend on  
722 differences in the chemical and photolysis mechanisms and the implementation of  
723 various physics schemes, all of which differ between the CTMs (see Colette et al.  
724 2017a). Specifically, the discrepancies found in the sensitivities of MDA8 O<sub>3</sub> to  
725 maximum temperature might be also attributed to biogenic emissions not prescribed in  
726 the models. This was particularly reflected in the analysis of the slopes ozone-  
727 temperature ( $m_{O_3-T}$ ) to assess the climate penalty, which differed between CTMs and  
728 regions when compared to the observations in both seasons. Most of the CTMs confirm  
729 the observed climate penalty in JAS, but with larger discrepancies in the external  
730 regions than in the internal regions. Furthermore, CTMs tend to overestimate the  
731 climate penalty in AMJ (particularly in the external regions).

732

733 Our results have shown discrepancies in the observed and simulated ozone sensitivities  
734 to relevant meteorological parameters for ozone formation and removal processes. In  
735 particular, we found that CTMs tend to overestimate the influence of maximum  
736 temperature and surface solar radiation in most of the regions, both strongly associated  
737 with ozone production. None of the CTMs captured the strength of the observed  
738 relationship between ozone and relative humidity appropriately, underestimating the  
739 effect of relative humidity, a key factor in the ozone removal processes. We speculate  
740 that ozone dry deposition schemes used by the CTMs in this study may not adequately  
741 represent the relationship between humidity and stomatal conductance, thus  
742 underestimating the ozone sink due to stomatal uptake. Further sensitivity analyses  
743 would be recommended for testing the impact of the current dry deposition schemes in  
744 the CTMs.

745

746 **Data availability**

747

748 The data are available upon request from the corresponding author.

749

750 **Acknowledgments**

751

752 We acknowledge Jordan L. Schnell for providing the interpolated dataset of MDA 8 O<sub>3</sub>.  
753 Modelling data used in the present analysis were produced in the framework of the  
754 EURODELTA-Trends Project initiated by the Task Force on Measurement and  
755 Modelling of the Convention on Long Range Transboundary Air Pollution.  
756 EURODELTA-Trends is coordinated by INERIS and involves modelling teams of  
757 BSC, CERE, CIEMAT, ENEA, IASS, JRC, MET Norway, TNO, SMHI. The views  
758 expressed in this study are those of the authors and do not necessarily represent the  
759 views of EURODELTA-Trends modelling teams. The MATCH participation was partly  
760 funded by the Swedish Environmental Protection Agency through the research program  
761 Swedish Clean Air and Climate (SCAC) and NordForsk through the research  
762 programme Nordic WelfAir (grant no. 75007).

763

764

765

766

767

768

769

770

771

772

773

774

775

776

777

778

779

780

781

782

783

784

785

786

787

788 **List of Tables:**



**Table 1.** Summary of the chemistry-transport models used in the study and the main characteristics (adapted from Colette et al. 2017).

Model	Meteorological driver	Research group	Vertical layers (vl) Vertical extent (ve) Surface concentration (sc) Depth first layer (dl)	Biogenic VOC	Dry deposition (dd) Stomatal resistance (sr)	Land use database(lu) Advection scheme (ad) Vertical diffusion (vd)
CHIMERE	WRF (common driver)	INERIS	<b>vl:</b> 9 sigma <b>ve:</b> surface to 500 hPa <b>sc:</b> First model level <b>dl:</b> 20m	MEGAN model v2.1 with highresolution spatial and temporal leaf area index (LAI; Yuan et al., 2011) and recomputed emissions factors based on the land use (Guenther et al., 2006)	<b>dd:</b> Resistance model (Emberson et al., 2000a, b) <b>sr:</b> Emberson et al. (2000a, b)	<b>lu:</b> GLOBCOVER (24 classes) <b>ad:</b> van Leer (1984) <b>vd:</b> vertical diffusion coefficient (Kz) approach following Troen and Mahrt (1986)
EMEP	WRF (common driver)	MET Norway	<b>vl:</b> 20 sigma <b>ve:</b> surface to 100 hPa <b>sc:</b> Downscaled to 3 m <b>dl:</b> 90m	Online emissions based upon maps of 115 species from Koeble and Seufert (2001), and hourly temperature and light using Guenther et al. (1993, 1994). See Simpson et al. (1995, 2012)	<b>dd:</b> Resistance model for gases (Venkatram and Pleim, 1999); for aerosols: Simpson et al. (2012) <b>sr:</b> DO3SEEMEP: Emberson et al. (2000a, b), Tuovinen et al. (2004), Simpson et al. (2012)	<b>lu:</b> CCE/SEI for Europe, elsewhere GLC2000 <b>ad:</b> Bott (1989) <b>vd:</b> Kz approach following O'Brien (1970) and Jeriřceviřc et al. (2010)
LOTOS-EUROS	RACMO2	TNO	<b>vl:</b> 5 (4 dynamic layers and a surface layer) <b>ve:</b> 5000 m <b>sc:</b> Downscaled to 3 m <b>dl:</b> 25m	Based upon maps of 115 species from Koeble and Seufert (2001), and hourly temperature and light (Guenther et al., 1991, 1993). See Beltman et al. (2013)	<b>dd:</b> Resistance model, DEPAC3.11 for gases, Van Zanten et al. (2010) and Zhang et al. (2001) for aerosols <b>rs:</b> Emberson et al. (2000a, b)	<b>lu:</b> Corine Land Cover 2000 (13 classes) <b>ad:</b> Walcek (2000) <b>vd:</b> Kz approach Yamartino et al. (2004)
MATCH	HIRLAM EURO4M	SMHI	<b>vl:</b> 39 hybrid levels of the meteorological model layers <b>ve:</b> surface to ca. 5000 m (4700–6000 m) <b>sc:</b> Downscaled to 3 m <b>dl:</b> ca. 60m	Online emissions based on Simpson et al. (2012), dependent on hourly temperature and light	<b>dd:</b> Resistance model depending on aerodynamic resistance and land use (vegetation). Similar to Andersson et al. (2007) <b>sr:</b> Simple, seasonally varying, diurnal variation of surface resistance for gases with stomatal resistance (similar to Andersson et al., 2007 and Simpson et al., 2012)	<b>lu:</b> CCE/SEI for Europe <b>ad:</b> Fourth-order massconserved advection scheme based on Bott (1989) <b>vd:</b> Implicit mass conservative Kz approach (see Robertson et al., 1999); Boundary layer parameterisation as detailed in Robertson et al. (1999) forms the basis for vertical diffusion and dry deposition
MINNI	WRF (common driver)	ENEA/Arianet S.r.l	<b>vl:</b> 16 fixed terrain-following layers <b>ve:</b> 10 000m <b>sc:</b> First model level <b>dl:</b> 40m	MEGAN v2.04 (Guenther et al., 2006)	<b>dd:</b> Resistance model based on Wesely (1989) <b>sr:</b> Wesely (1989)	<b>lu:</b> Corine Land Cover 2006 (22 classes) <b>ad:</b> Blackman cubic polynomials (Yamartino,1993) <b>vd:</b> Kz approach following Lange (1989)

791  
792

Predictor	Definition	793
LO3	Lag of MDA8 O <sub>3</sub> (24 h)	794
Tx	Maximum temperature	795
RH	Relative humidity	796
SSRD	Surface solar radiation	797
Wdir	Wind direction	798
W10m	Wind speed	799
day	$\sin(2\pi d_t/365.25)$ ,	800
	$\cos(2\pi d_t/365.25)$	801
		802

803  
804  
805  
806

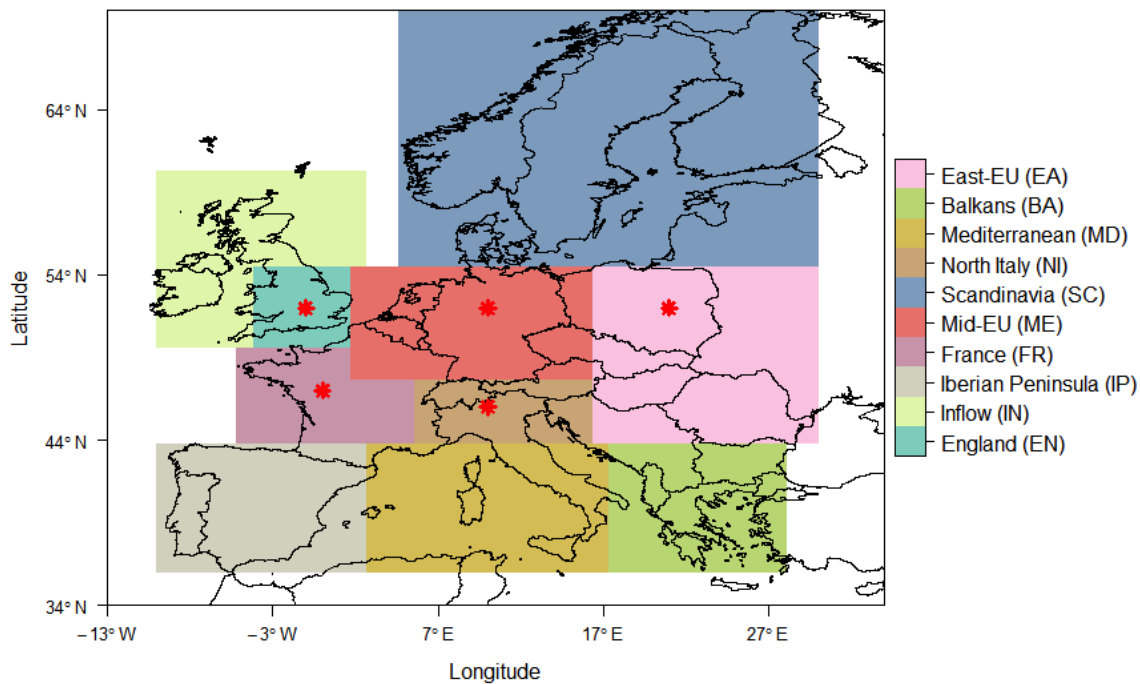
**Table 2.** List of the predictors used in the multiple linear regression analysis: meteorological parameters, lag of MDA8 O<sub>3</sub> (24h, previous day) and the seasonal cycle components.

Region	Acronym	Coordinates (longitude, latitude)	807
England	EN	5W-2E, 50N-55N	808
Inflow	IN	10W-5W, 50N-60N, and 5W-2E, 55N-60N	809
Iberian Peninsula	IP	10W-3E, 36N-44N	810
France	FR	5W-5E, 44N-50N	811
Mid-Europe	ME	2E-16E, 48N-55N	812
Scandinavia	SC	5E-16E, 55N-70N	813
North Italy	NI	5E-16E, 44N-48N	814
Balkans	BA	18E-28E, 38N-44N	815
Mediterranean	MD	3E-18E, 36N-44N	816
Eastern Europe	EA	16E-30E, 44N-55N	817
			818
			819
			820
			821

822  
823  
824  
825  
826  
827  
828  
829  
830  
831  
832  
833  
834  
835  
836  
837  
838  
839  
840  
841  
842  
843

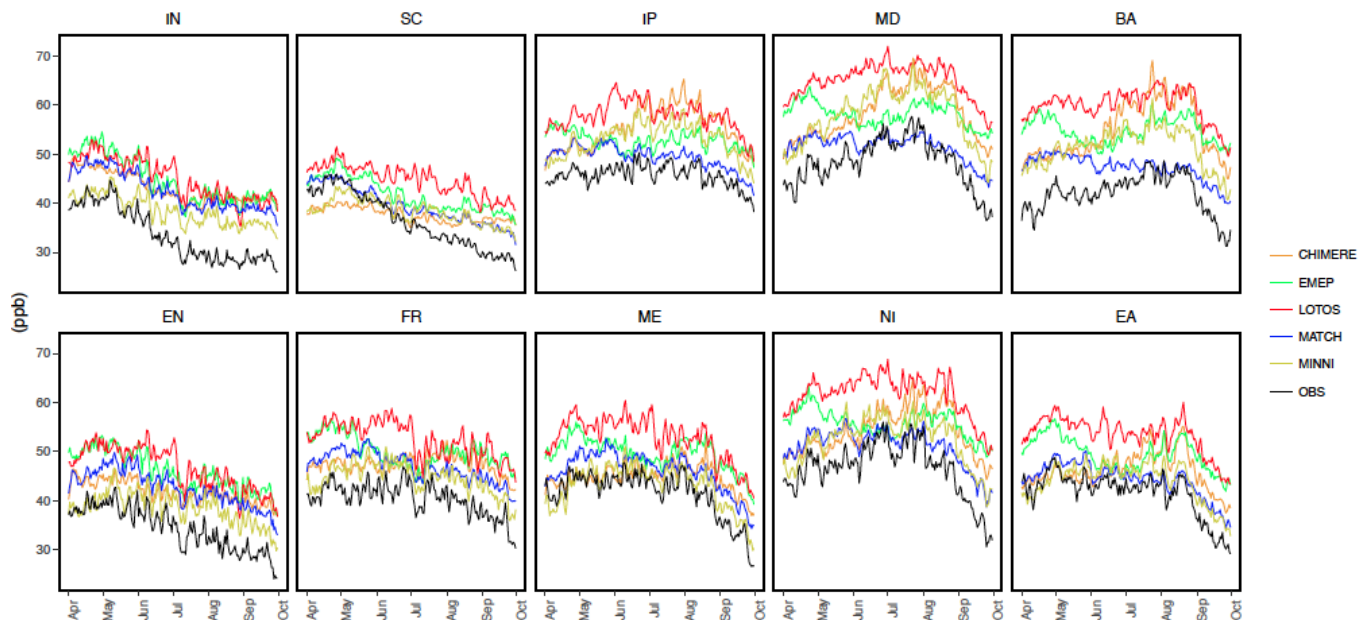
**Table 3.** List of the regions with the short name and the coordinates.

844 **List of Figures:**  
 845



846  
 847  
 848  
 849  
 850  
 851  
 852

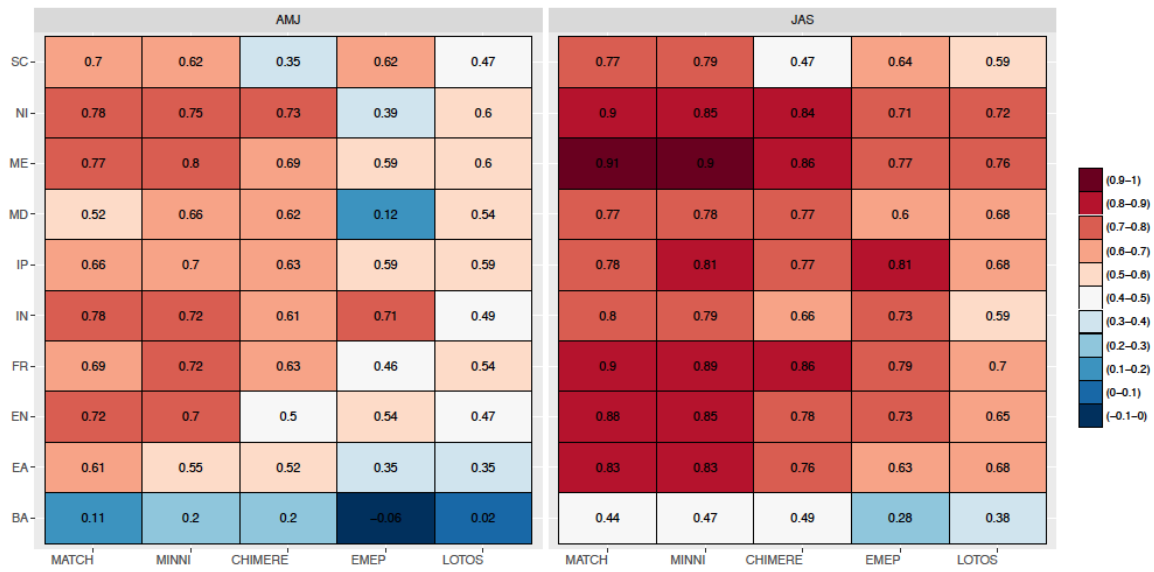
**Figure 1.** Map of the regions considered in the study. Regions indicated with a black star are referred to the internal regions in the text. The rest of regions are referred to the external regions of the European domain.



853  
 854  
 855  
 856  
 857

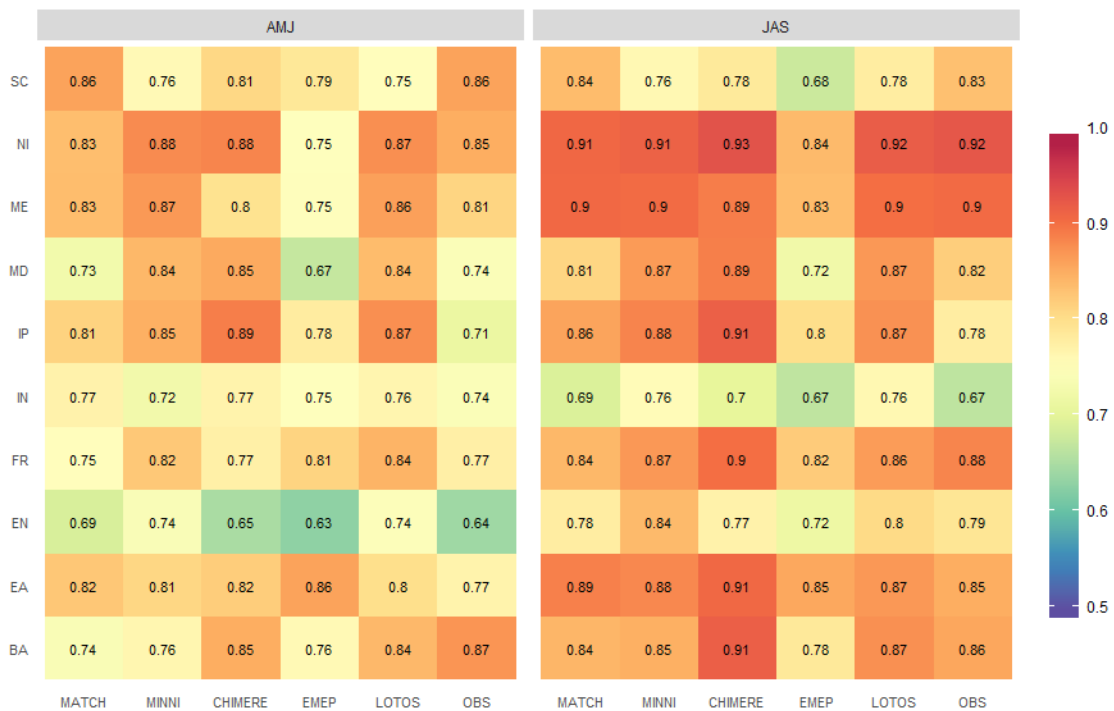
**Figure 2.** Time series of daily averages of MDA8 O<sub>3</sub> during the ozone season (April-September) for the period of study (2000-2010) at each subregion.

858  
859



860  
861  
862  
863  
864  
865  
866

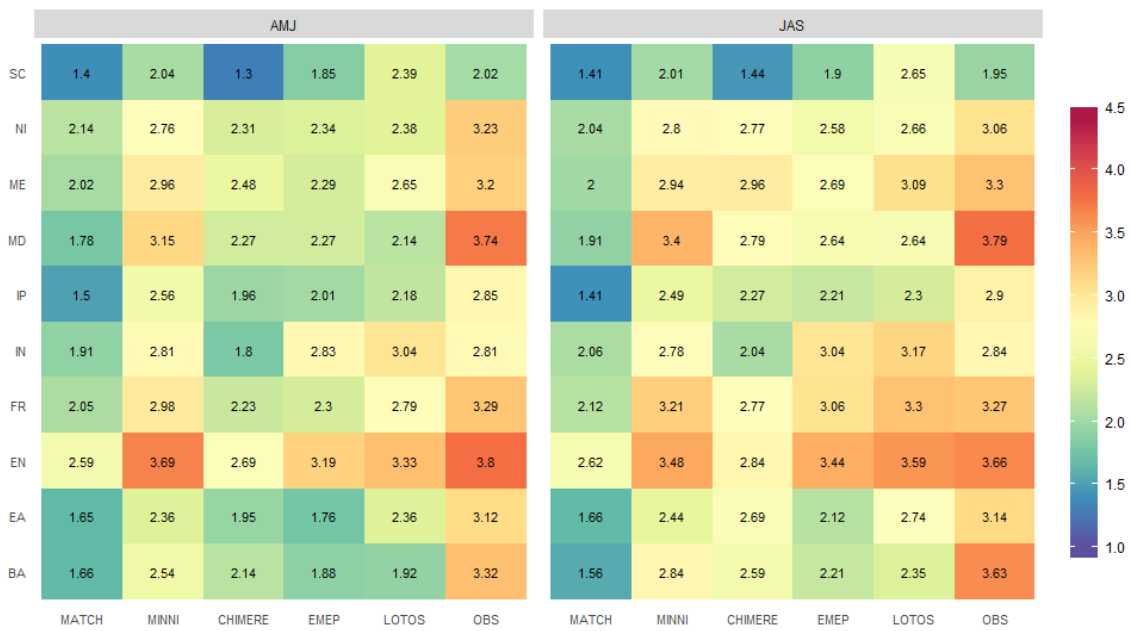
**Figure 3.** Correlation coefficients between observed and modelled MDA8 O<sub>3</sub> for spring (AMJ) and summer (JAS) for the period of study (2000-2010) at each region (rows) and model (columns, ordered by highest correlation values).



867  
868  
869  
870  
871  
872  
873  
874  
875  
876  
877

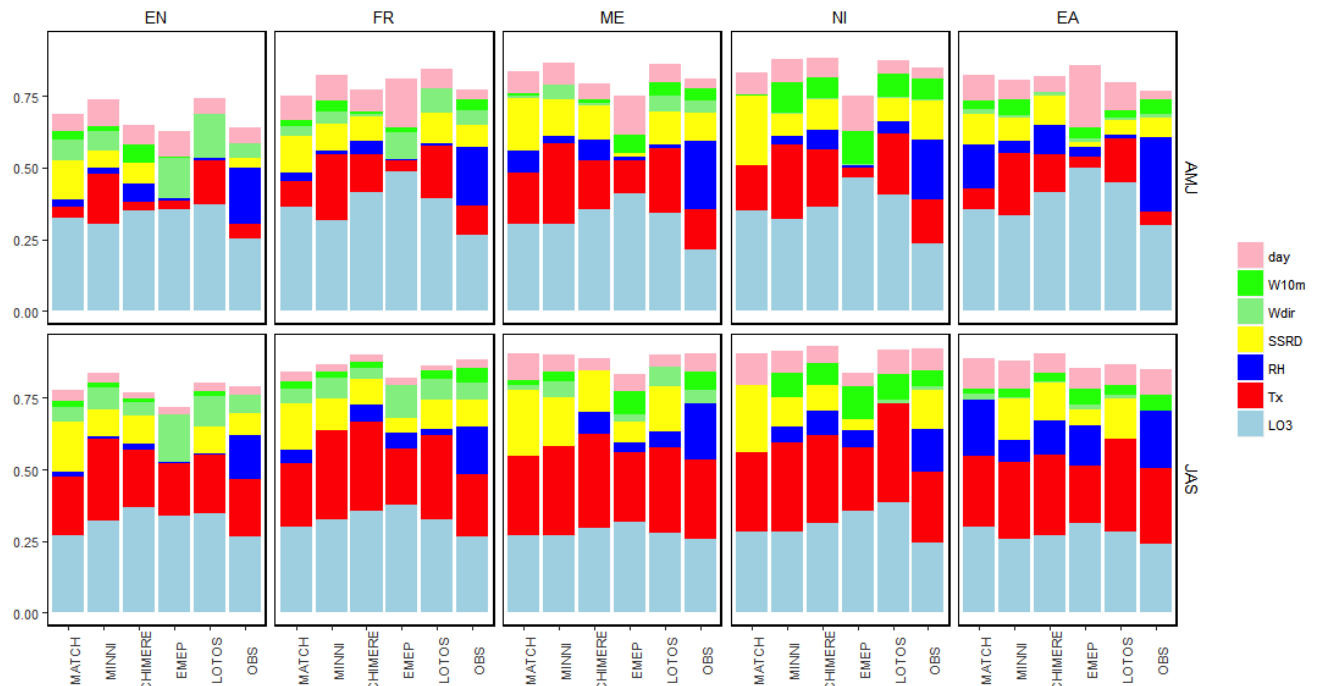
**Figure 4.** Coefficients of determination ( $R^2$ ) for each CTM-based (ordered as in Fig.3) and observation-based MLR in spring (AMJ) and summer (JAS).

878  
879



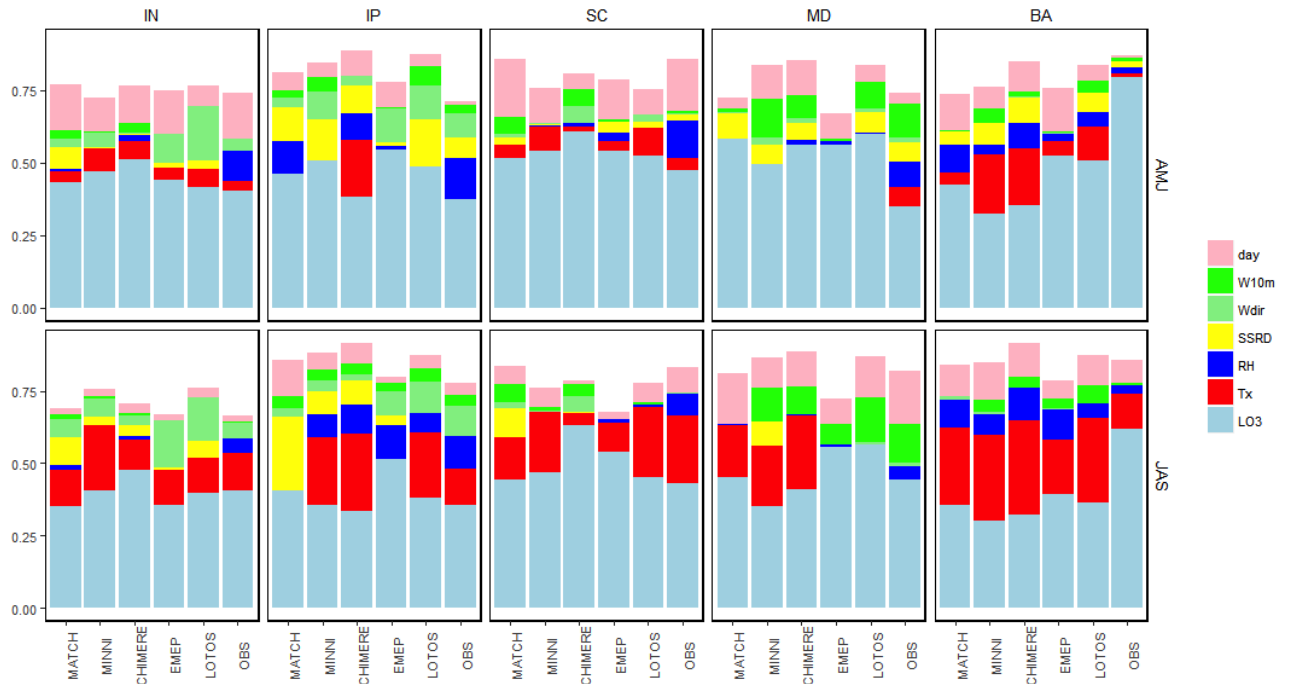
880  
881  
882  
883  
884  
885  
886

**Figure 5.** Root mean square errors (RMSE) for each CTM-based (ordered as in Fig.3) and observation-based MLR at each region, in spring (AMJ) and summer (JAS).



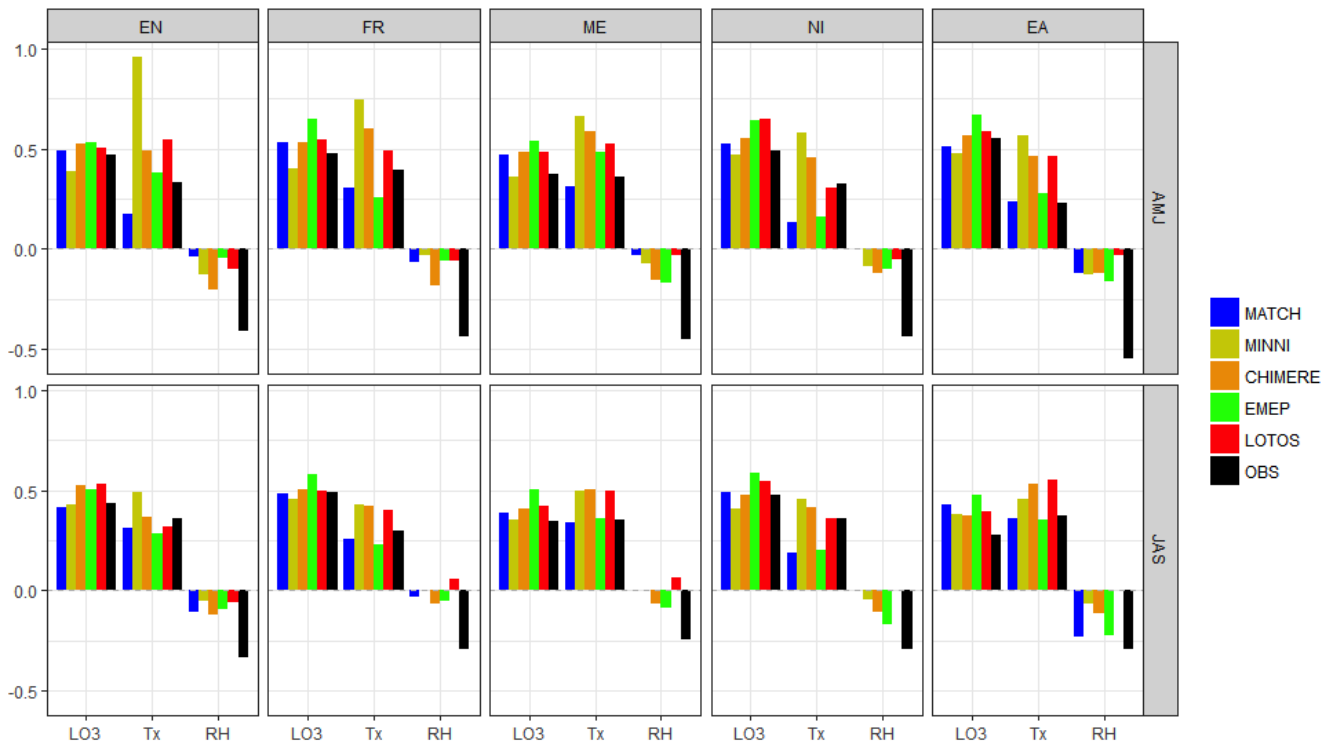
887  
888  
889  
890  
891  
892

**Figure 6.** Proportion of each predictor to the total explained variance for each CTM-based (ordered as in Fig.3) and observation-based MLR in AMJ (top) and JAS (bottom) for the internal regions: England (EN), France (FR), Mid-Europe (ME), North Italy (NI) and East-Europe (EA).



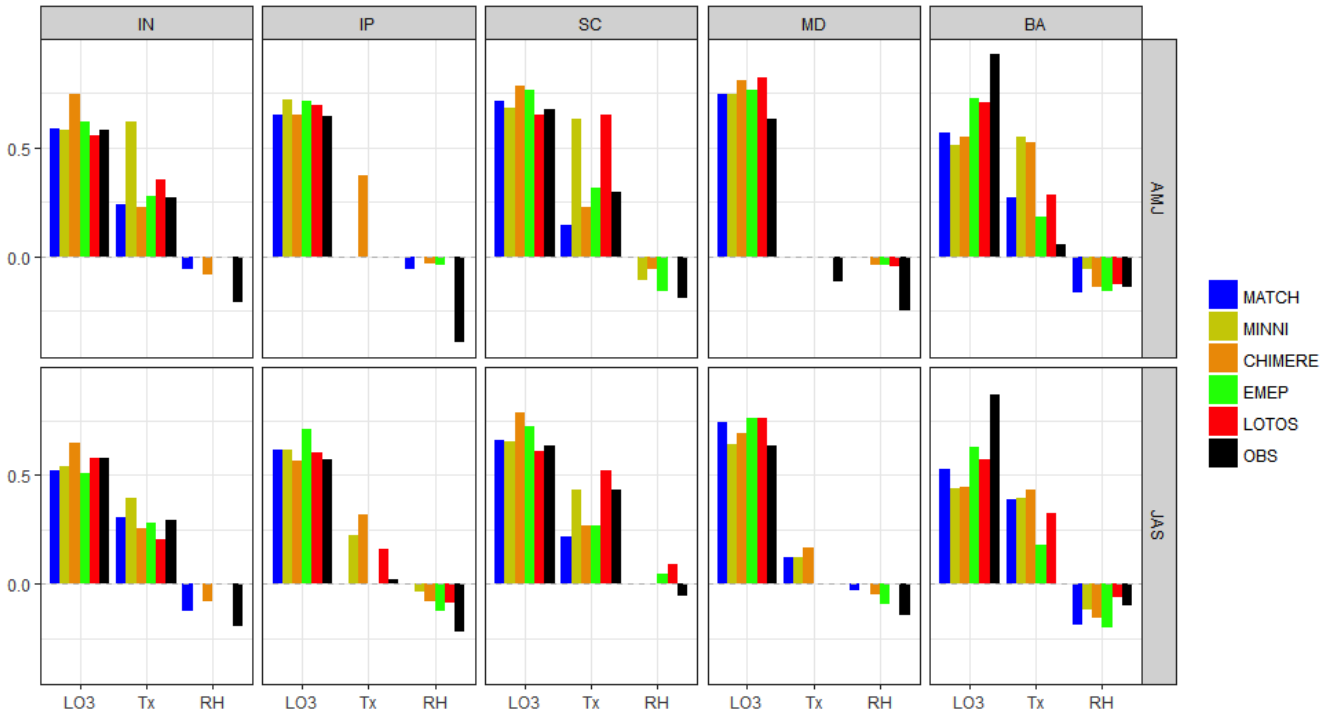
894  
895  
896  
897  
898  
899  
900

**Figure 7.** Proportion of each predictor to the total explained variance for each CTM-based (ordered as in Fig.3) and observation-based MLR in AMJ (top) and JAS (bottom) for the external regions: Inflow (IN), Iberian Peninsula (IP), Scandinavia (SC), Mediterranean (ME) and Balkans (BA).



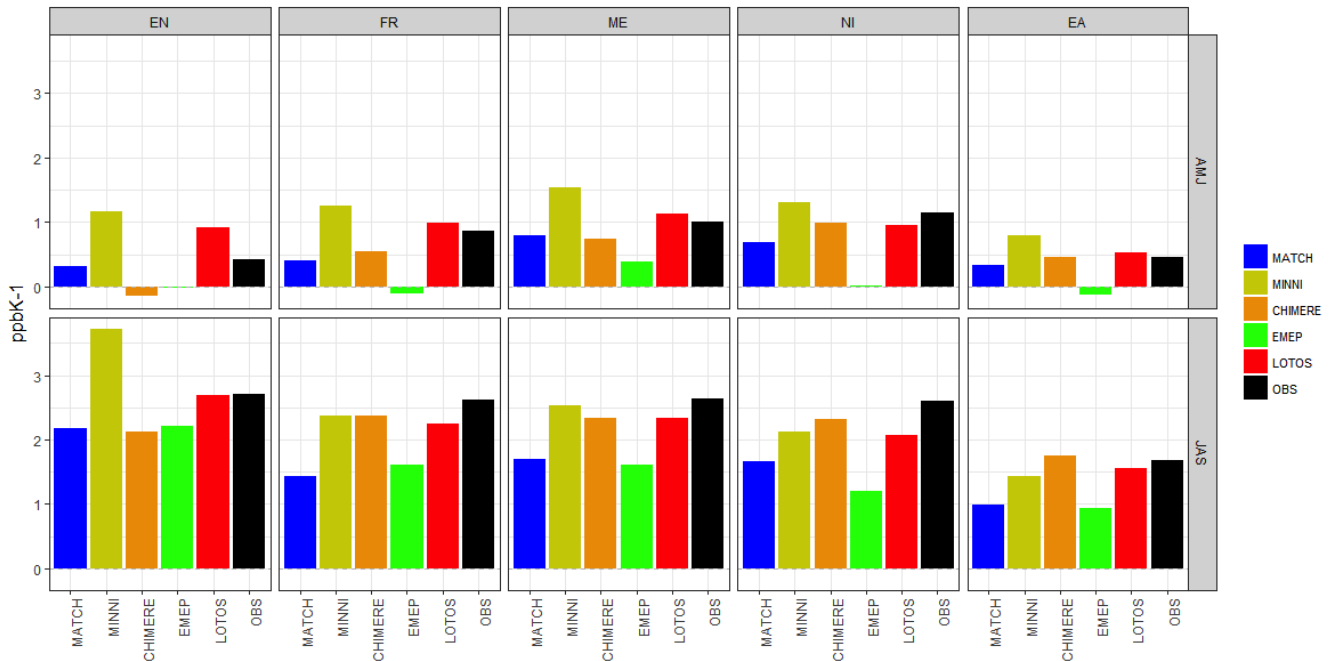
901  
902  
903  
904  
905  
906

**Figure 8.** Standardised coefficients values of the main key-driving factors (LO3, Tx and RH) for each CTM-based (ordered as in Fig.3) and observation-based MLR in AMJ (top) and JAS (bottom) and for the internal regions: England (EN), France (FR), Mid-Europe (ME), North Italy (NI) and East-Europe (EA).



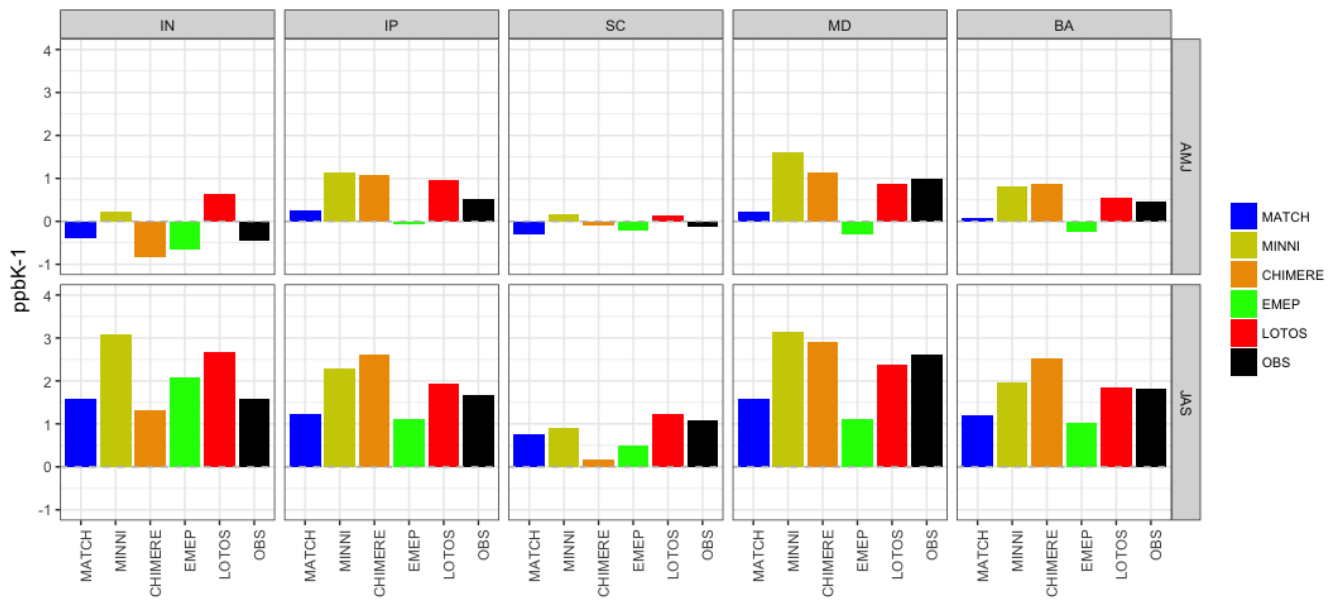
908  
909  
910  
911  
912  
913  
914

**Figure 9.** Standardised coefficients values of the main key-driving factors (LO3, Tx and RH) for each CTM-based (ordered as in Fig.3) and observation-based MLR in AMJ (top) and JAS (bottom) and for the external regions: Inflow (IN), Iberian Peninsula (IP), Scandinavia (SC), Mediterranean (ME) and Balkans (BA).



915  
916  
917  
918  
919  
920

**Figure 10.** Slopes ( $m_{O_3-T}$ ; ppbK<sup>-1</sup>) obtained from a simple linear regression to estimate the relationship ozone-temperature for each CTM-based (ordered as in Fig.3) and observation-based MLR in AMJ (top) and JAS (bottom) and for the internal regions: England (EN), France (FR), Mid-EU (ME), North Italy (NI), East-EU (EA).



921  
 922  
 923  
 924  
 925  
 926  
 927

**Figure 11.** Slopes ( $m_{O_3-T}$ ;  $ppbK^{-1}$ ) obtained from a simple linear regression to estimate the relationship ozone-temperature for each CTM-based (ordered as in Fig.3) and observation-based MLR in AMJ (top) and JAS (bottom) and for the external regions: Inflow (IN), Iberian Peninsula (IP), Scandinavia (SC), Mediterranean (ME) and Balkans (BA).



928

929 **References**

930

931 Andersson, C., J. Langner, and R. Bergström: Interannual variation and trends in air  
932 pollution over Europe due to climate variability during 1958–2001 simulated with a  
933 regional CTM coupled to the ERA-40 reanalysis, *Tellus, Ser. B*, 59, 77–98, 2007.

934

935 Andersson C., Bergström R., Johansson C., Population exposure and mortality due to  
936 regional background PM in Europe–Long-term simulations of source region and  
937 shipping contributions, *Atmospheric Environment*, 43, 22, 3614-3620,  
938 <http://dx.doi.org/10.1016/j.atmosenv.2009.03.040>, 2009.

939

940 Andersson, C. and Engardt, M.: European ozone in a future climate: Importance of  
941 changes in dry deposition and isoprene emissions, *J. Geophys. Res.-Atmos.*, 115,  
942 D02303, doi:10.1029/2008jd011690, 2010.

943

944 Baklanov, A., Schlünzen, K., Suppan, P., Baldasano, J., Brunner, D., Aksoyoglu, S.,  
945 Carmichael, G., Douros, J., Flemming, J., Forkel, R., Galmarini, S., Gauss, M., Grell,  
946 G., Hirtl, M., Joffre, S., Jorba, O., Kaas, E., Kaasik, M., Kallos, G., Kong, X.,  
947 Korsholm, U., Kurganskiy, A., Kushta, J., Lohmann, U., Mahura, A., Manders-Groot,  
948 A., Maurizi, A., Moussiopoulos, N., Rao, S. T., Savage, N., Seigneur, C., Sokhi, R. S.,  
949 Solazzo, E., Solomos, S., Sørensen, B., Tsegas, G., Vignati, E., Vogel, B., and Zhang,  
950 Y.: Online coupled regional meteorology chemistry models in Europe: current status  
951 and prospects, *Atmos. Chem. Phys.*, 14, 317–398, doi:10.5194/acp-14-317-2014, 2014.

952

953 Barrero M A, Grimalt J O and Canton L.: Prediction of daily ozone concentration  
954 maxima in the urban atmosphere *Chemometr. Intell. Lab. Syst.* 80 67–76, 2005.

955

956 Beltman, J. B., Hendriks, C., Tum, M., and Schaap, M.: The impact of large scale  
957 biomass production on ozone air pollution in Europe, *Atmos. Environ.*, 71, 352–363,  
958 2013.

959

960 Bessagnet, B., Pirovano, G., Mircea, M., Cuvelier, C., Aulinger, A., Calori, G., Ciarelli,  
961 G., Manders, A., Stern, R., Tsyro, S., García Vivanco, M., Thunis, P., Pay, M.-T.,  
962 Colette, A., Couvidat, F., Meleux, F., Rouïl, L., Ung, A., Aksoyoglu, S., Baldasano, J.  
963 M., Bieser, J., Briganti, G., Cappelletti, A., D’Isidoro, M., Fi- nardi, S., Kranenburg, R.,  
964 Silibello, C., Carnevale, C., Aas, W., Dupont, J.-C., Fagerli, H., Gonzalez, L., Menut,  
965 L., Prévôt, A. S. H., Roberts, P., and White, L.: Presentation of the EURODELTA III  
966 intercomparison exercise – evaluation of the chemistry transport models’ performance  
967 on criteria pollutants and joint analysis with meteorology, *Atmos. Chem. Phys.*, 16,  
968 12667–12701, doi:10.5194/acp-16-12667-2016, 2016.

969

970 Bloomfield P J, Royle J A, Steinberg L J and Yang Q: Accounting for meteorological  
971 effects in measuring urban ozone levels and trends *Atmos. Environ.* 30 3067–77, 1996 .

972

973 Bloomer, B. J., Stehr, J. W., Piety, C. A., Salawitch, R. J., and Dickerson, R. R.:  
974 Observed relationships of ozone air pollution with temperature and emissions, *Geophys.*  
975 *Res. Lett.*, 36, L09803, doi:10.1029/2009gl037308, 2009.

976

977 Bott, A.: A Positive Definite Advection Scheme Obtained by Nonlinear  
978 Renormalization of the Advective Fluxes, *Mon. Weather Rev.*, 117, 1006–1015, 1989.  
979

980 Brown-Steiner, B., Hess, P. G., and Lin, M. Y.: On the capabilities and limitations of  
981 GCM simulations of summertime regional air quality: A diagnostic analysis of ozone  
982 and temperature simulations in the US using CESM CAM-Chem, *Atmos. Environ.*, 101,  
983 134–148, doi:10.1016/j.atmosenv.2014.11.001, 2015.  
984

985 Brunner, D., Jorba, O., Savage, N., Eder, B., Makar, P., Giordano, L., Badia, A.,  
986 Balzarini, A., Baro, R., Bianconi, R., Chemel, C., Forkel, R., Jimenez-Guerrero, P.,  
987 Hirtl, M., Hodzic, A., Honzak, L., Im, U., Knote, C., Kuenen, J. J. P., Makar, P. A.,  
988 MandersGroot, A., Neal, L., Perez, J. L., Pirovano, G., San Jose, R., Savage, N.,  
989 Schroder, W., Sokhi, R. S., Syrakov, D., Torian, A., Werhahn, K., Wolke, R., van  
990 Meijgaard, E., Yahya, K., Zabkar, R., Zhang, Y., Zhang, J., Hogrefe, C., and Galmarini,  
991 S.: Comparative analysis of meteorological performance of coupled chemistry-  
992 meteorology models in the context of AQMEII phase 2, *Atmos. Environ.*, 115, 470–  
993 498, 2015.  
994

995 Camalier, L., Cox, W., and Dolwick, P.: The effects of meteorology on ozone in urban  
996 areas and their use in assessing ozone trends, *Atmos. Environ.*, 41, 7127–7137, 2007.  
997

998 Carro-Calvo, L., C. Ordóñez, R. García-Herrera, J. L. Schnell: Spatial clustering and  
999 meteorological drivers of summer ozone in Europe, *Atmos. Environ.*, 167, 496-  
1000 510, <https://doi.org/10.1016/j.atmosenv.2017.08.050>, 2017.  
1001

1002 Chaloulakou A, Saisana M and Spyrellis N: Comparative assessment of neural networks  
1003 and regression models for forecasting summertime ozone in Athens *Science of the Total  
1004 Environment* 313 1–13, 2003.  
1005

1006 Coates, J., Mar, K. A., Ojha, N., and Butler, T. M.: The influence of temperature on  
1007 ozone production under varying NO<sub>x</sub> conditions – a modelling study, *Atmos. Chem.  
1008 Phys.*, 16, 11601-11615, <https://doi.org/10.5194/acp-16-11601-2016>, 2016.  
1009

1010 Colette, A., Andersson, C., Baklanov, A., Bessagnet, B., Brandt, J., Christensen, J.,  
1011 Doherty, R., Engardt, M., Geels, C., Giannakopoulos, C., Hedegaard, G., Katragkou, E.,  
1012 Langner, J., Lei, H., Manders, A., Melas, D., Meleux, F., Rouil, L., Sofiev, M., Soares,  
1013 J., Stevenson, D., Tombrou-Tzella, M., Varotsos, K., and Young, P.: Is the ozone  
1014 climate penalty robust in Europe?, *Environ. Res. Lett.*, 10, 084015, doi:10.1088/1748-  
1015 9326/10/8/084015, 2015.  
1016

1017 Colette, A., Andersson, C., Manders, A., Mar, K., Mircea, M., Pay, M.-T., Raffort, V.,  
1018 Tsyro, S., Cuvelier, C., Adani, M., Bessagnet, B., Bergström, R., Briganti, G., Butler,  
1019 T., Cappelletti, A., Couvidat, F., D'Isidoro, M., Doumbia, T., Fagerli, H., Granier, C.,  
1020 Heyes, C., Klimont, Z., Ojha, N., Otero, N., Schaap, M., Sindelarova, K., Stegehuis, A.  
1021 I., Roustan, Y., Vautard, R., van Meijgaard, E., Vivanco, M. G., and Wind, P.:  
1022 EURODELTA-Trends, a multi-model experiment of air quality hindcast in Europe over  
1023 1990–2010, *Geosci. Model Dev. Discuss.*, <https://doi.org/10.5194/gmd-2016-309>,  
1024 accepted, 2017a.  
1025

1026 Colette, A., Solberg, S., Beauchamp, M., Bessagnet, B., Malherbe, L., and Guerreiro,

1027 C.: Long term air quality trends in Europe: Contribution of meteorological variability,  
1028 natural factors and emissions, ETC/ACM, Bilthoven, 2017b.

1029

1030 Comrie A. C.: Comparing neural networks and regression models for ozone forecasting  
1031 J. Air Waste Manage. Assoc. 47 653–63, 1997.

1032

1033 Dahlgren, P., Landelius, T., Kållberg, P., and Gollvik, S.: A high-resolution regional  
1034 reanalysis for Europe. Part 1: Three-dimensional reanalysis with the regional HIgh-  
1035 Resolution Limited-Area Model (HIRLAM), Quarterly Journal of the Royal  
1036 Meteorological Society, 142, 2119-2131, 10.1002/qj.2807, 2016.

1037

1038 Davis, J., Cox, W., Reff, A., Dolwick, P.: A comparison of Cmaq-based and  
1039 observation-based statistical models relating ozone to meteorological parameters.  
1040 Atmospheric Environment 45, 3481e3487. [http://dx.doi.org/10.1016/](http://dx.doi.org/10.1016/J.Atmosenv.2010.12.060)  
1041 [J.Atmosenv.2010.12.060](http://dx.doi.org/10.1016/J.Atmosenv.2010.12.060), 2011.

1042 Dawson, J.P., Adams, P.J., Pandis, S.N.: Sensitivity of ozone to summertime climate in  
1043 the Eastern USA: a modeling case study. Atmos. Environ. 41, 1494– 1511, 2007.

1044

1045 Dawson, J. P., Racherla, P. N., Lynn, B. H., Adams, P. J., and Pan- dis, S. N.:  
1046 Simulating present-day and future air quality as cli- mate changes: model evaluation,  
1047 Atmos. Environ., 42, 4551– 4566, doi:10.1016/j.atmosenv.2008.01.058, 2008.

1048

1049 Dee D P et al. :The ERA-Interim reanalysis: configuration and performance of the data  
1050 assimilation system Quart. J. R. Meteorol. Soc. 137 553–97, 2001.

1051

1052 Doherty, R. M., Wild, O., Shindell, D. T., Zeng, G., MacKenzie, I. A., Collins, W. J.,  
1053 Fiore, A. M., Stevenson, D. S., Dentener, F. J., Schultz, M. G., Hess, P., Derwent, R.  
1054 G., and Keating, T. J.: Impacts of climate change on surface ozone and intercontinental  
1055 ozone pollution: a multi- model study, J. Geophys. Res.-Atmos., 118, 3744–3763,  
1056 doi:10.1002/jgrd.50266, 2013.

1057

1058 Emberson, L. D., Ashmore, M. R., Simpson, D., Tuovinen, J.-P., and Cambridge, H.  
1059 M.: Towards a model of ozone deposition and stomatal uptake over Europe, Norwegian  
1060 Meteorological Institute, Oslo, Norway, 57, 2000a.

1061

1062 Emberson, L. D., Ashmore, M. R., Simpson, D., Tuovinen, J.-P., and Cambridge, H.  
1063 M.: Modelling stomatal ozone flux across Europe, Water Air Soil Pollut., 109, 403–413,  
1064 2000b.

1065

1066 Elminir H.K.: Dependence of urban air pollutants on meteorology, Science of The Total  
1067 Environment, 350,225-237, <http://dx.doi.org/10.1016/j.scitotenv.2005.01.043>, 2005.

1068

1069 Fischer M., Rust H.W., and Ulbrich U.: Seasonality in extreme precipitation – using  
1070 extreme value statistics to describe the annual cycle in german daily precipitation.  
1071 Meteorol. Z. accepted, 2017.

1072

1073 Fiore, A. M., Dentener, F. J., Wild, O., Cuvelier, C., Schultz, M. G., Hess, P., Textor,  
1074 C., Schulz, M., Doherty, R. M., Horowitz, L. W., MacKenzie, I. A., Sanderson, M. G.,  
1075 Shindell, D. T., Stevenson, D. S., Szopa, S., Van Dingenen, R., Zeng, G., Atherton, C.,

1076 Bergmann, D., Bey, I., Carmichael, G., Collins, W. J., Duncan, B. N., Faluvegi, G.,  
1077 Folberth, G., Gauss, M., Gong, S., Hauglustaine, D., Holloway, T., Isaksen, I. S. A.,  
1078 Jacob, D. J., Jonson, J. E., Kaminski, J. W., Keating, T. J., Lupu, A., Marmer, E.,  
1079 Montanaro, V., Park, R. J., Pitari, G., Pringle, K. J., Pyle, J. A., Schroeder, S., Vivanco,  
1080 M. G., Wind, P., Wojcik, G., Wu, S., and Zuber, A.: Multimodel estimates of  
1081 intercontinental source-receptor relationships for ozone pollution, *J. Geophys. Res.-*  
1082 *Atmos.*, 114, D04301, doi:10.1029/2008jd010816, 2009.

1083

1084 Fix, M. J., D. Cooley, A. Hodzic, E. Gilleland, B. T. Russell, W. C. Porter, and G. G.  
1085 Pfister, 2018: Observed and predicted sensitivities of extreme surface ozone to  
1086 meteorological drivers in three US cities. *Atmospheric Environment*, 176, 292-300,  
1087 doi:10.1016/j.atmosenv.2017.12.036.

1088 Gan C., Hogrefe C., Mathur R., Pleim J., Xing J., Wong D., Gilliam R., Pouliot G., Wei  
1089 C.: Assessment of the effects of horizontal grid resolution on long-term air quality  
1090 trends using coupled WRF-CMAQ simulations, *Atmospheric Environment*, 132, 207-  
1091 216,1352-2310,https://doi.org/10.1016/j.atmosenv.2016.02.036., 2016.

1092

1093 Grell, G. A., Peckham, S. E., Schmitz, R., McKeen, S. A., Frost, G., Skamarock, W. C.,  
1094 and Eder, B.: Fully coupled “online” chemistry within the WRF model, *Atmospheric*  
1095 *Environment*, 39, 6957-6975, http://dx.doi.org/10.1016/j.atmosenv.2005.04.027, 2005.

1096

1097 Grömping U.: Estimators of relative importance in linear regression based on variance  
1098 decomposition *Am. Stat.* 61 139–47, 2007.

1099

1100 Guenther, A., Zimmerman, P., Harley, P., Monson, R., and Fall, R.: Isoprene and  
1101 monoterpene rate variability: model evaluations and sensitivity analyses, *J. Geophys.*  
1102 *Res.*, 98, 12609–12617, 1993.

1103

1104 Guenther, A., Zimmerman, P., and Wildermuth, M.: Natural volatile organic compound  
1105 emission rate estimates for US woodland landscapes, *Atmos. Environ.*, 28, 1197–1210,  
1106 1994.

1107

1108 Guenther, A., Karl, T., Harley, P., Wiedinmyer, C., Palmer, P. I., and Geron, C.:  
1109 Estimates of global terrestrial isoprene emissions using MEGAN (Model of Emissions  
1110 of Gases and Aerosols from Nature), *Atmos. Chem. Phys.*, 6, 3181–3210,  
1111 doi10.5194/acp-6-3181-2006, 2006.

1112

1113 Hedegaard, G. B., Christensen, J. H., and Brandt, J.: The relative importance of impacts  
1114 from climate change vs. emissions change on air pollution levels in the 21st century,  
1115 *Atmos. Chem. Phys.*, 13, 3569-3585, doi:10.5194/acp-13-3569-2013, 2013.

1116

1117 Hendriks C., Forsell N., Kiesewetter G., Schaap M., Schöpp W.: Ozone concentrations  
1118 and damage for realistic future European climate and air quality scenarios, *Atmospheric*  
1119 *Environment*, 144, 208-219, http://dx.doi.org/10.1016/j.atmosenv.2016.08.026, 2016.

1120

1121 Hodnebrog, Ø., Solberg, S., Stordal, F., Svendby, T. M., Simpson, D., Gauss, M.,  
1122 Hilboll, A., Pfister, G. G., Turquety, S., Richter, A., Burrows, J. P., and Denier van der  
Gon, H. A. C.: Impact of forest fires, biogenic emissions and high temperatures on the

1123 elevated Eastern Mediterranean ozone levels during the hot summer of 2007, *Atmos.*  
1124 *Chem. Phys.*, 12, 8727-8750, <https://doi.org/10.5194/acp-12-8727-2012>, 2012  
1125  
1126 Hogrefe, C., Biswas, J., Lynn, B., Civerolo, K., Ku, J. Y., Rosenthal, J., Rosenzweig,  
1127 C., Goldberg, R., and Kinney, P. L.: Simulating regional-scale ozone climatology over  
1128 the eastern United States: model evaluation results, *Atmos. Environ.*, 38, 2627–2638,  
1129 2004.  
1130  
1131 IPCC, Climate Change 2013, the Physical Science Basis. Working Group I contribution  
1132 to the fifth assessment report of the Intergovernmental Panel on Climate  
1133 Change, Cambridge University Press, 2013.  
1134  
1135 Jacob, D. J. and Winner, D. A.: Effect of climate change on air quality, *Atmos.*  
1136 *Environ.*, 43, 51–63, doi:10.1016/j.atmosenv.2008.09.051, 2009.  
1137  
1138 Jericevic, A., Kraljevic, L., Grisogono, B., Fagerli, H., and Vecenaj, Ž.:  
1139 Parameterization of vertical diffusion and the atmospheric boundary layer height  
1140 determination in the EMEP model, *Atmos. Chem. Phys.*, 10, 341–364,  
1141 <https://doi.org/10.5194/acp-10-341-2010>, 2010.  
1142  
1143 Jonson, J. E., Simpson, D., Fagerli, H., and Solberg, S.: Can we explain the trends in  
1144 European ozone levels?, *Atmos. Chem. Phys.*, 6, 51–66, doi:10.5194/acp-6-51-2006,  
1145 2006.  
1146  
1147 Kavassalis, S. C., and J. G. Murphy: Understanding ozone-meteorology correlations: A  
1148 role for dry deposition, *Geophys. Res. Lett.*, 44, 2922–2931,  
1149 doi:10.1002/2016GL071791, 2017.  
1150  
1151 Koeble, R. and Seufert, G.: Novel Maps for Forest Tree Species in Europe, A Changing  
1152 Atmosphere, 8th European Symposium on the Physico-Chemical Behaviour of  
1153 Atmospheric Pollutants, Torino, Italy, 2001.  
1154  
1155 Kong, X., Forkel R., Sokhi R. S., Suppan P., Baklanov A., Gauss M., Brunner D., Barò  
1156 R., Balzarini A., Chemel C., Curci G., Jiménez-Guerrero P., Hirtl M., Honzak L., Im U.,  
1157 Pérez J. L., Pirovano G., San Jose R., Schlünzen K. H. , Tsegas G., Tuccella P.,  
1158 Werhahn J., Žabkar R., Galmarini S.: Analysis of Meteorology-Chemistry Interactions  
1159 During Air Pollution Episodes Using Online Coupled Models within AQMEII Phase-2,  
1160 *Atmospheric Environment*, <http://dx.doi.org/10.1016/j.atmosenv.2014.09.020>., 2014.  
1161  
1162 Kutner M. H., Nachtsheim C. J. and Neter J.: *Applied Linear Regression Models* 4th Ed  
1163 (Boston, MA: McGraw-Hill Irwin) 2004.  
1164  
1165 Lange, R.: Transferrability of a three-dimensional air quality model between two  
1166 different sites in complex terrain, *J. Appl. Meteorol.*, 78, 665–679, 1989.  
1167  
1168 Langner, J., Bergström R. and Foltescu V.: Impact of climate change on surface ozone  
1169 and deposition of sulphur and nitrogen in Europe, *Atmos. Environ.*, 39, 1129–1141,  
1170 doi:10.1016/j.atmosenv.2004.09.082, 2005.  
1171  
1172 Lelieveld, J., and P. J. Crutzen: Influence of cloud and photochemical processes on

1172 tropospheric ozone, *Nature*, 343, 227–233, 1990.

1173 Lemaire, V. E. P., Colette, A. and Menut, L.: Using statistical models to explore  
1174 ensemble uncertainty in climate impact studies: the example of air pollution in Europe,  
1175 *Atmos. Chem. Phys.*, 16, 2559–2574, doi:10.5194/acp-16-2559-2016, 2016.

1176

1177 Lindeman R.H. , Merenda P. F. and Gold RZ: *Introduction to Bivariate and Multivariate*  
1178 *Analysis*. Scott, Foresman, Glenview, IL, 1980.

1179

1180 Linderson M. L.: Objective classification of atmospheric circulation over southern  
1181 Scandinavia *Int. J. Climatol.* 21 155–69, 2001.

1182

1183 Mailler, S., Menut, L., Khvorostyanov, D., Valari, M., Couvidat, F., Siour, G.,  
1184 Turquety, S., Briant, R., Tuccella, P., Bessagnet, B., Colette, A., Létinois, L., Markakis,  
1185 K., and Meleux, F.: CHIMERE-2017: from urban to hemispheric chemistry-transport  
1186 modeling, *Geosci. Model Dev.*, 10, 2397–2423, [https://doi.org/10.5194/gmd-10-2397-](https://doi.org/10.5194/gmd-10-2397-2017)  
1187 2017, 2017.

1188 Maindonald J, Braun J: *Data analysis and graphics using R: an example-based*  
1189 *approach*.Cambridge (United Kingdom), Cambridge University Press, 2006.

1190

1191 Makar, P.A., Gong,W., Hogrefe, C., Zhang, Y., Curci, G., Zakbar, R., Milbrandt, J., Im,  
1192 U., Galmarini, S., Gravel, S., Zhang, J., Hou, A., Pabla, B., Cheung, P., Bianconi, R.,  
1193 2015b. Feedbacks between Air Pollution and Weather, Part 1: Effects on Weather.  
1194 *Atmos. Environ.* 115, 442e469.

1195

1196 Manders, A. M. M., van Meijgaard, E., Mues, A. C., Kranenburg, R., van Ulft, L. H.,  
1197 and Schaap, M.: The impact of differences in large-scale circulation output from climate  
1198 models on the regional modeling of ozone and PM, *Atmos. Chem. Phys.*, 12, 9441–  
1199 9458, doi:10.5194/acp-12-9441-2012, 2012.

1200

1201 Manders, A. M. M., Builtjes, P. J. H., Curier, L., Denier van der Gon, H. A.  
1202 C., Hendriks, C., Jonkers, S., Kranenburg, R., Kuenen, J., Segers, A. J.,  
1203 Timmermans, R. M. A., Visschedijk, A., Wichink Kruit, R. J., Van Pul, W. A. J.,  
1204 Sauter, F. J., van der Swaluw, E., Swart, D. P. J., Douros, J., Eskes, H., van  
1205 Meijgaard, E., van Ulft, B., van Velthoven, P., Banzhaf, S., Mues, A., Stern, R.,  
1206 Fu, G., Lu, S., Heemink, A., van Velzen, N., and Schaap, M.: Curriculum Vitae of  
1207 the LOTOS-EUROS (v2.0) chemistry transport model, *Geosci. Model Dev. Discuss.*,  
1208 <https://doi.org/10.5194/gmd-2017-88>, in review, 2017.

1209

1210 Meijgaard, E. v., van Ulft, L. H., Lenderink, G., de Roode, S. R., Wipfler, L., Boers, R.,  
1211 and Timmermans, R. M. A.: Refinement and application of a regional atmospheric  
1212 model for climate scenario calculations of Western Europe, *KvR 054/12*, 44, 2012.

1213

1214 Meleux, F., Solmon, F., and Giorgi, F.: Increase in summer European ozone amounts  
1215 due to climate change, *Atmos. Environ.*, 41, 7577–7587,  
1216 doi:10.1016/j.atmosenv.2007.05.048, 2007.

1217

1218 Millán, M. M., Sanz, M. J., Salvador, R., and Mantilla, E.: Atmospheric dynamics and  
1219 ozone cycles related to nitrogen deposition in the western Mediterranean, *Environ.*

1220 Pollut., 118, 167–186, 2002.  
1221  
1222 Mills, G., Hayes, F., Jones, M. L. M., and Cinderby, S.: Identifying ozone-sensitive  
1223 communities of (semi-)natural vegetation suitable for mapping exceedance of critical  
1224 levels, *Environ. Pollut.*, 146, 736–743, doi:10.1016/j.envpol.2006.04.005, 2007.  
1225  
1226 Mircea, M., Grigoras, G., D’Isidoro, M., Righini, G., Adani, M., Briganti, G.,  
1227 Ciancarella, L., Cappelletti, A., Calori, G., Cionni, I., Cremona, G., Finardi, S., Larsen,  
1228 B. R., Pace, G., Perrino, C., Piersanti, A., Silibello, C., Vitali, L., and Zanini, G.: Impact  
1229 of grid resolution on aerosol predictions: a case study over Italy, *Aerosol and Air*  
1230 *Quality Research*, 1253–1267, doi: 10.4209/aaqr.2015.02.0058, 2016.  
1231  
1232 Monks, P. S.: A review of the observations and origins of the spring ozone maximum,  
1233 *Atmos. Environ.*, 34, 3545–3561, 2000.  
1234  
1235 Monks, P. S., Archibald, A. T., Colette, A., Cooper, O., Coyle, M., Derwent, R.,  
1236 Fowler, D., Granier, C., Law, K. S., Mills, G. E., Stevenson, D. S., Tarasova, O.,  
1237 Thouret, V., von Schneidmesser, E., Sommariva, R., Wild, O., and Williams, M. L.:  
1238 Tropospheric ozone and its precursors from the urban to the global scale from air  
1239 quality to short-lived climate forcer, *Atmos. Chem. Phys.*, 15, 8889-8973,  
1240 <https://doi.org/10.5194/acp-15-8889-2015>, 2015.  
1241  
1242 O’Brien, J. J.: A note on the vertical structure of the eddy Exchange coefficient in the  
1243 planetary boundary layer, *J. Atmos. Sci.*, 27, 1213–1215, 1970.  
1244  
1245 Ordóñez, C., Mathis, H., Furger, M., Henne, S., Hoglin, C., Staehelin, J., Prevot,  
1246 A.S.H.: Changes of daily surface ozone maxima in Switzerland in all seasons from 1992  
1247 to 2002 and discussion of summer 2003. *Atmos. Chem. Phys.* 5, 1187– 1203, 2005.  
1248  
1249 Ordóñez, C., Barriopedro, D., García-Herrera, R., Sousa, P. M., and Schnell, J. L.:  
1250 Regional responses of surface ozone in Europe to the location of high-latitude blocks  
1251 and subtropical ridges, *Atmos. Chem. Phys.*, 17, 3111-3131,  
1252 <https://doi.org/10.5194/acp-17-3111-2017>, 2017.  
1253  
1254 Otero, N., Sillmann, J., Schnell, J.L., Rust, H.W., Butler, T., 2016. Synoptic and  
1255 meteorological drivers of extreme ozone concentrations over Europe. *Environ. Res.*  
1256 *Lett.* 11 (2), 24005. <http://dx.doi.org/10.1088/1748-9326/11/2/024005>.  
1257  
1258 Porter W C, Heald C L, Cooley D and Russell B 2015 Investigating the observed  
1259 sensitivities of air quality extremes to meteorological drivers via quantile regression  
1260 *Atmos. Chem. Phys. Discuss.* 15 10349–66, 2015.  
1261  
1262 Pusede S E et al. : On the temperature dependence of organic reactivity, nitrogen  
1263 oxides, ozone production, and the impact of emission controls in San Joaquin Valley,  
1264 California *Atmos. Chem. Phys.* 14 3373–95, 2014.  
1265  
1266 Querol, X., Gangoiti, G., Mantilla, E., Alastuey, A., Minguillón, M. C., Amato, F.,  
1267 Reche, C., Viana, M., Moreno, T., Karanasiou, A., Rivas, I., Pérez, N., Ripoll, A.,  
1268 Brines, M., Ealo, M., Pandolfi, M., Lee, H.-K., Eun, H.-R., Park, Y.-H., Escudero, M.,  
1269 Beddows, D., Harrison, R. M., Bertrand, A., Marchand, N., Lyasota, A., Codina, B.,

1270 Olid, M., Udina, M., Jiménez-Esteve, B., Soler, M. R., Alonso, L., Millán, M., and Ahn,  
1271 K.-H.: Phenomenology of high-ozone episodes in NE Spain, *Atmos. Chem. Phys.*, 17,  
1272 2817-2838, <https://doi.org/10.5194/acp-17-2817-2017>, 2017.  
1273

1274 Rasmussen, D. J., Fiore, A. M., Naik, V., Horowitz, L. W., McGinnis, S. J., and  
1275 Schultz, M. G.: Surface ozone-temperature relationships in the eastern US: A monthly  
1276 climatology for evaluating chemistry-climate models, *Atmos. Environ.*, 47, 142–153,  
1277 doi:10.1016/j.atmosenv.2011.11.021, 2012.  
1278

1279 Robertson, L., Langner, J., and Engardt, M.: An Eulerian Limited-Area Atmospheric  
1280 Transport Model, *Journal of Applied Meteorology*, 38, 190-210, 1999.  
1281

1282 Rust H, Maraun D. and Osborn T.: Modelling seasonality in extreme precipitation *Eur.*  
1283 *Phys. J. Special Topics* 174 99–111, 2009.  
1284

1285 Rust H. W., Vrac M., Sultan B., and Lengaigne M.: Mapping weather-type influence on  
1286 Senegal precipitation based on a spatial-temporal statistical model. *J. Climate*, 26:8189–  
1287 8209. ISSN 0894-8755. URL <http://dx.doi.org/10.1175/JCLI-D-12-00302.1.1>. 2013  
1288

1289 Schaap, M., Timmermans, R. M. A., Roemer, M., Boersen, G. A. C., Builtjes, P.,  
1290 Sauter, F., Velders, G., and Beck, J.: The LOTOS-EUROS model: description,  
1291 validation and latest developments, *International Journal of Environment and Pollution*,  
1292 32, 270-290, 2008.  
1293

1294 Schaap M., Cuvelier C, Hendriks C., Bessagnet B., Baldasano J.M., Colette A., Thunis  
1295 P., Karam D., Fagerli H., Graff A., Kranenburg R., Nyiri A., Pay M.T., Rouil L., Schulz  
1296 M., Simpson D., Stern R., Terrenoire E., Wind P.: Performance of European chemistry  
1297 transport models as function of horizontal resolution, *Atmospheric Environment*, 112,  
1298 90-105, <http://dx.doi.org/10.1016/j.atmosenv.2015.04.003>, 2015.  
1299

1300 Skamarock, W. C., Klemp, J. B., Dudhia, J., Gill, D. O., Barker, D. M., Duda, M. G.,  
1301 Huang, X. Y., Wang, W., and Powers, J. G.: A Description of the Advanced Research  
1302 WRF Version 3, NCAR, 2008.  
1303

1304 Schnell, J. L., Holmes, C. D., Jangam, A., and Prather, M. J.: Skill in forecasting  
1305 extreme ozone pollution episodes with a global atmospheric chemistry model, *Atmos.*  
1306 *Chem. Phys.*, 14, 7721–7739, doi:10.5194/acp-14-7721-2014, 2014.  
1307

1308 Schnell, J. L., Prather, M. J., Josse, B., Naik, V., Horowitz, L. W., Cameron-Smith, P.,  
1309 Bergmann, D., Zeng, G., Plummer, D. A., Sudo, K., Nagashima, T., Shindell, D. T.,  
1310 Faluvegi, G., and Strode, S. A.: Use of North American and European air quality  
1311 networks to evaluate global chemistry–climate modeling of surface ozone, *Atmos.*  
1312 *Chem. Phys.*, 15, 10581-10596, doi:10.5194/acp-15-10581-2015, 2015.  
1313

1314 Seo, J., Youn, D., Kim, J. Y., and Lee, H.: Extensive spatiotemporal analyses of surface  
1315 ozone and related meteorological variables in South Korea for the period 1999–2010,  
1316 *Atmos. Chem. Phys.*, 14, 6395-6415, <https://doi.org/10.5194/acp-14-6395-2014>, 2014.  
1317

1318 Sillman, S. and Samson, P.J: Impact of temperature on oxidant photochemistry in  
1319 urban, polluted rural and remote environments. *Journal of Geophysical Research* 100:



1320 doi: 10.1029/94JD02146. issn: 0148-0227, 1995.

1321

1322 Simpson, D., Guenther, A., Hewitt, C., and Steinbrecher, R.: Biogenic emissions in  
 1323 Europe 1. Estimates and uncertainties, *J. Geophys. Res.*, 100, 22875–22890, 1995.

1324

1325 Simpson, D., Benedictow, A., Berge, H., Bergström, R., Emberson, L. D., Fagerli, H.,  
 1326 Flechard, C. R., Hayman, G. D., Gauss, M., Jonson, J. E., Jenkin, M. E., Nyíri, A.,  
 1327 Richter, C., Semeena, V. S., Tsyro, S., Tuovinen, J.-P., Valdebenito, Á., and Wind, P.:  
 1328 The EMEP MSC-W chemical transport model – technical description, *Atmos. Chem.*  
 1329 *Phys.*, 12, 7825–7865, <https://doi.org/10.5194/acp-12-7825-2012>, 2012

1330

1331 Simpson, D., Andersson, C., Christensen, J. H., Engardt, M., Geels, C., Nyiri, A.,  
 1332 Posch, M., Soares, J., Sofiev, M., Wind, P., and Langner, J.: Impacts of climate and  
 1333 emission changes on nitrogen deposition in Europe: a multi-model study, *Atmos. Chem.*  
 1334 *Phys.*, 14, 6995-7017, <https://doi.org/10.5194/acp-14-6995-2014>, 2014.

1335

1336 Smyth, S., Yin, D., Roth, H., Jiang, W., Moran, M.D., Crevier, L.P., 2006. The impact  
 1337 of GEM and MM5 meteorology on CMAQ air quality modeling results in eastern  
 1338 Canada and the northeastern United States. *Journal of Applied Meteorology* 45,  
 1339 1525e1541. doi:10.1175/JAM2420.1.

1340

1341 Solberg, S., R. G. Derwent, Ø. Hov, J. Langner, and A. Lindskog: European abatement  
 1342 of surface ozone in a global perspective, *Ambio*, 34, 47–53, 2005.

1343

1344 Solberg, S., Hov, Ø., Sovde, A., Isaksen, I. S. A., Coddeville, P., De Backer, H.,  
 1345 Forster, C., Orsolini, Y., and Uhse, K.: European surface ozone in the extreme summer  
 1346 2003, *J. Geophys. Res. Atmos.*, 113, D07307, doi:10.1029/2007jd009098, 2008.

1347

1348 Solberg, S., Colette, A., and Guerreiro, C. B. B.: Discounting the impact of meteorology  
 1349 to the ozone concentration trends. ETC/ACM, NILU, INERIS.  
 1350 <https://doi.org/10.13140/rg.2.2.15389.92649>, 2016.

1351

1352 Steiner, A.L., Tonse, S., Cohen, R.C., Goldstein, A.H., Harley, R.A.: Influence of  
 1353 future climate and emissions on Regional air quality in California. *Journal of*  
 1354 *Geophysical Research-Atmospheres* 111, 2006.

1355

1356 Vautard, R., Honore, C., Beekmann, M., and Rouil, L.: Simulation of ozone  
 1357 during the August 2003 heat wave and emission control scenarios, *Atmos.*  
 1358 *Environ.*, 39, 2957–2967, doi:10.1016/j.atmosenv.2005.01.039, 2005.

1359

1360 Tang L., Chen D.L., Karlsson P.E., Gu Y.F., Ou T.H. Synoptic circulation and its  
 1361 influence on spring and summer surface ozone concentrations in Southern Sweden  
 1362 *Boreal Environment Research*, 14, 889-902, 2009.

1363

1364 Tarasova, O. A., Brenninkmeijer, C. A. M., Jöckel, P., Zvyagintsev, A. M., and  
 1365 Kuznetsov, G. I.: A climatology of surface ozone in the extra tropics: cluster analysis of  
 1366 observations and model results, *Atmos. Chem. Phys.*, 7, 6099–6117, doi:10.5194/acp-7-  
 1367 6099-2007, 2007.

1368

1369 Thompson M L, Reynolds J, Cox L H, Guttorp P and Sampson P D: A review of

1370 statistical methods for the meteorological adjustment of tropospheric ozone *Atmos.*  
1371 *Environ.* 35 617–30, 2001.

1372

1373 Troen, I. and Mahrt, L.: A simple model of the atmospheric boundary layer: Sensitivity  
1374 to surface evaporation, *Bound.-Lay. Meteorol.*, 37, 129–148, 1986.

1375

1376 Tuovinen, J.-P., Ashmore, M., Emberson, L., and Simpson, D.: Testing and improving  
1377 the EMEP ozone deposition module, *Atmos. Environ.*, 38, 2373–2385, 2004.

1378

1379 van Loon, M., Vautard, R., Schaap, M., Bergström, R., Bessagnet, B., Brandt, J.,  
1380 Bultjes, P. J. H., Christensen, J. H., Cuvelier, C., Graff, A., Jonson, J. E., Krol, M.,  
1381 Langner, J., Roberts, P., Rouil, L., Stern, R., Tarrasón, L., Thunis, P., Vignati, E.,  
1382 White, L., and Wind, P.: Evaluation of long-term ozone simulations from seven regional  
1383 air quality models and their ensemble, *Atmospheric Environment*, 41, 2083–2097, 2007.

1384

1385 Vautard, R., Moran, M.D., Solazzo, E., Gilliam, R.C., Matthias, V., Bianconi, R.,  
1386 Chemel, C., Ferreira, J., Geyer, B., Hansen, A.B., Jericevic, A., Prank, M., Segers, A.,  
1387 Silver, J.D., Werhahn, J., Wolke, R., Rao, S.T., Galmarini, S., 2012. Evaluation of the  
1388 meteorological forcing used for the Air Quality Model Evaluation International  
1389 Initiative (AQMEII) air quality simulations. *Atmos. Environ.* 53, 15e37.

1390

1391 van Leer, B.: Multidimensional explicit difference schemes for hyperbolic conservation  
1392 laws, in: *Computing Methods in Applied Sciences and Engineering VI*, edited by:  
1393 Lions, R. G. A. J. L., Elsevier, Amsterdam, 1984.

1394

1395 Van Zanten, M. C., Sauter, F. J., Wichink Kruit, R. J., Van Jaarsveld, J. A., and Van Pul,  
1396 W. A. J.: Description of the DEPAC module: 75 Dry deposition modelling with  
1397 DEPAC\_GC2010, Bilthoven, the Netherlands, 2010.

1398

1399 Walcek, C. J.: Minor flux adjustment near mixing ratio extremes for simplified yet  
1400 highly accurate monotonic calculation of tracer advection, *J. Geophys. Res.*, 105, 9335–  
1401 9348, 2000.

1402

1403 Wesely, M. L.: Parameterization of surface resistances to gaseous dry deposition in  
1404 regional-scale numerical models, *Atmos. Environ.*, 23, 1293–1304, 1989.

1405

1406 Wilson, R. C., Fleming, Z. L., Monks, P. S., Clain, G., Henne, S., Konovalov, I. B.,  
1407 Szopa, S., and Menut, L.: Have primary emission reduction measures reduced ozone  
1408 across Europe? An analysis of European rural background ozone trends 1996–2005,  
1409 *Atmos. Chem. Phys.*, 12, 437–54, <https://doi.org/10.5194/acp-12-437-2012>, 2012.

1410

1411 Wu, S., Mickley, L. J., Leibensperger, E. M., Jacob, D. J., Rind, D., and Streets, D. G.:  
1412 Effects of 2000–2050 global change on ozone air quality in the United States, *J.*  
1413 *Geophys. Res.-Atmos.*, 113, D18312, doi:10.1029/2007JD009639, 2008.

1414

1415 Yamartino, R. J., J. Flemming, and R.M. Stern: Adaptation of analytic diffusivity  
1416 formulations to Eulerian grid model layers of finite thickness. In *27th ITM on Air*  
1417 *Pollution Modelling and its Application*. Banff, Canada. 2004.

1418

1419 Yuan, H., Dai, Y., Xiao, Z., Ji, D., and Shangguan, W.: Reprocessing the MODIS Leaf

- 1420 Area Index Products for Land Surface and Climate Modelling, *Remote Sens. Environ.*,  
1421 155, 1171–1187, <https://doi.org/10.1016/j.rse.2011.01.001>, 2011.  
1422
- 1423 Zhang, L., Gong, S., Padro, J., and Barrie, L.: A size-segregated particle dry deposition  
1424 scheme for an atmospheric aerosol module, *Atmos. Environ.*, 35, 549–560, 2001.  
1425
- 1426 Zhang, Y.: Online-coupled meteorology and chemistry models: his- tory, current status,  
1427 and outlook, *Atmos. Chem. Phys.*, 8, 2895– 2932, doi:10.5194/acp-8-2895-2008, 2008.  
1428